Mathematical Biosciences 393 (2026) 109609

Contents lists available at ScienceDirect

Mathematical Biosciences

journal homepage: www.elsevier.com/locate/mbs

Original research article

# Predator-prey dynamics with personality-dependent foraging and maturation delay: stability switches, Hopf and Bogdanov-Takens bifurcations

Heping Jiang [a], Shan Gao [b,c], Hao Wang [b,c,*]

[a] School of Mathematics and Statistics, Huangshan University, Anhui, 245041, China
[b] Department of Mathematical and Statistical Sciences, University of Alberta, Edmonton, Alberta, T6G 2G1, Canada
[c] Interdisciplinary Lab for Mathematical Ecology & Epidemiology, University of Alberta, Edmonton, Alberta, T6G 2G1, Canada

ARTICLE INFO

*Keywords:*
Predator-prey
Personality heterogeneity
Maturation delay
Stability switches
Bogdanov-Takens
Global Hopf branches

ABSTRACT

Individual differences in predator boldness can alter encounter and attack rates, while maturation introduces biologically realistic time lags. We couple these two mechanisms in a Rosenzweig-MacArthur framework by modeling a nonlinear, personality-dependent attack rate and deriving a stage-structured maturation delay for predators, yielding a delay differential equation system. For the delay-free model, we establish positivity and boundedness, characterize boundary and interior equilibria, and provide a complete local bifurcation picture: transcritical and saddle-node bifurcations together with Hopf bifurcations that generate stable cycles; at codimension two, we prove the occurrence of cusp/Bogdanov-Takens points with accompanying homoclinic loops. Introducing maturation delay produces delay-induced complexity: multiple stability switches, sequences of Hopf bifurcations on distinct frequency branches, and global Hopf continua that connect critical delays. Analytical predictions are corroborated numerically via continuation (DDE-BIFTOOL), revealing periodic and quasi-periodic oscillations as well as bistability between coexistence and boundary states. Our results identify personality heterogeneity and developmental timing as interacting drivers of oscillatory and multistable dynamics, and provide parameter thresholds, expressed in biologically interpretable combinations, for when coexistence equilibria lose or regain stability. These findings refine theory for delayed predator-prey interactions and suggest targets (e.g., handling/harvest and juvenile survival) for stabilizing management in systems with behavioral variation.

## 1. Introduction

Predator-prey interactions are foundational to community dynamics, ecosystem stability, and biodiversity. Predators can reshape prey population trajectories by altering survival, growth, behaviour, size structure, and spatial distribution, while prey availability reciprocally regulates predator populations [1–6]. A central theoretical framework for these interactions is the Rosenzweig-MacArthur (RM) model, which couples logistic prey growth with a Holling type II functional response [7–10]:

$$\begin{cases} \dfrac{du(t)}{dt} = r\,u(t)\left(1-\dfrac{u(t)}{K}\right) - \dfrac{\beta\,u(t)\,v(t)}{1+\beta h\,u(t)}, \\ \dfrac{dv(t)}{dt} = n\,\dfrac{\beta\,u(t)\,v(t)}{1+\beta h\,u(t)} - m\,v(t), \end{cases} \tag{1.1}$$

where $u(t)$ and $v(t)$ denote prey and predator densities, respectively. Here $r$ is the prey intrinsic growth rate, $K$ the carrying capacity, $n$ the conversion efficiency, $\beta$ the attack rate, $h$ the handling time, and $m$ the predator mortality rate. Despite its widespread use, the RM model omits two empirically supported features that can strongly modulate dynamics: (i) intraspecific behavioural variation among predators and (ii) biological time delays.

A common simplifying assumption in (1.1) is that all predators forage identically. This contradicts extensive evidence for consistent, individual-level behavioural differences within populations [11,12]. In particular, the boldness-shyness axis is repeatedly linked to foraging propensity and risk-taking [13,14], and has been documented across taxa, from terrestrial carnivores (wolves, African wild dogs) and birds to aquatic organisms [15–18]. Bold individuals typically accept higher risk and can achieve elevated encounter or attack rates relative to shy conspecifics, thereby altering trophic interactions and energy flux. Empirical work shows that predator behavioural type can systematically shift functional-response parameters [19], yet classical dynamical models rarely incorporate such personality-driven foraging differences.

* Corresponding author.
*E-mail addresses:* 104049@hsu.edu.cn (H. Jiang), sgao9@ualberta.ca (S. Gao), hao8@ualberta.ca (H. Wang).

https://doi.org/10.1016/j.mbs.2025.109609
Received 12 October 2025; Received in revised form 16 December 2025; Accepted 30 December 2025
Available online 7 January 2026

Many key life-history processes unfold over nontrivial time scales: maturation, gestation, and stage transitions introduce delays that can qualitatively change system behaviour [20,21]. Delay differential equations (DDEs) offer a natural way to represent these processes. Since the early introduction of delays into population models [22], numerous studies have shown that maturation lags can destabilize equilibria, generate sustained oscillations via Hopf bifurcation, and yield complex transient dynamics; related global Hopf structures have been analyzed in both single-species and predator–prey systems with Holling-type responses, as well as in epidemiological settings with stage structure [23–25]. Notably, delay-induced cycles may interact non-additively with other nonlinear mechanisms. How such delays couple with personality-driven foraging remains poorly understood.

Motivated by these gaps, we extend the RM framework by incorporating (i) a personality-dependent predator attack rate along the bold-shy spectrum and (ii) a fixed maturation delay derived from an age-structured predator cohort. The resulting delay differential predator-prey model captures within-population behavioural heterogeneity and ontogenetic timing. Our main contributions are listed below:

- For the delay-free model, we establish positivity and boundedness, classify boundary and interior equilibria, and provide a complete local bifurcation picture including transcritical, saddle-node, and Hopf bifurcations. At codimension two, we identify Bogdanov-Takens (cusp) points and associated global phenomena.
- With maturation delay, we determine the existence and stability of equilibria, derive delay-induced Hopf bifurcations and stability switches (including multiple switches when two frequency branches exist), and characterize global Hopf continua connecting critical delays. Analytical results are corroborated by numerical continuation.

The remaining paper is organized as follows. Section 2 formulates the personality-dependent functional response and introduces the maturation delay via a stage-structured derivation. Section 3 analyzes the corresponding no-delay system, including equilibrium classification, stability, and local/codimension-two bifurcations. Section 4 treats the delayed system, establishing stability of boundary states, deriving Hopf conditions and global Hopf branches, and documenting stability switches with numerical support. Section 5 summarizes ecological implications and outlines future directions.

## 2. Model derivation

Building on the Rosenzweig-MacArthur framework [9], Ahmed et al. [26] argued that consumers may take risky actions to maximize resource intake under fluctuating conditions and, consequently, the attack rate should be modeled as a state-dependent quantity rather than a fixed parameter. They proposed the predator-prey system:

$$\begin{cases} \dfrac{du(t)}{dt} = r\,u(t)\left(1-\dfrac{u(t)}{K}\right) - \dfrac{\beta(u(t),v(t))\,u(t)\,v(t)}{1+\beta(u(t),v(t))\,h\,u(t)}, \\ \dfrac{dv(t)}{dt} = n\,\dfrac{\beta(u(t),v(t))\,u(t)\,v(t)}{1+\beta(u(t),v(t))\,h\,u(t)} - m\,v(t), \end{cases} \tag{2.1}$$

with the nonlinear, personality-dependent attack rate

$$\beta(u(t),v(t)) \;=\; b_0 \;+\; \frac{a\,v(t)}{c\,u(t)+v(t)}. \tag{2.2}$$

Here $b_0>0$ is the minimum ("most shy") attack rate, $a>0$ is the maximum increment in attack rate due to boldness ("most bold"), and $c>0$ is a half-saturation constant that modulates how strongly boldness elevates the attack rate (smaller $c$ means stronger effect). From (2.2), one readily checks the monotonicity and bounds:

$$\partial_v\beta(u,v) = \frac{a\,c\,u}{(cu+v)^2} > 0,$$
$$\partial_u\beta(u,v) = -\frac{a\,c\,v}{(cu+v)^2} < 0, \qquad b_0 \le \beta(u,v) \le b_0 + a.$$

To incorporate a fixed maturation time, we embed an age structure for predators. Let $b(t,\alpha)$ denote the density of predators of age $\alpha\ge 0$ at time $t$. The population evolves according to

$$\partial_t b(t,\alpha) + \partial_\alpha b(t,\alpha) = -\mu(\alpha)\,b(t,\alpha), \qquad \mu(\alpha) = \begin{cases} \delta, & 0\le\alpha\le\tau, \\ m, & \alpha>\tau, \end{cases} \tag{2.3}$$

with boundary (birth) condition

$$b(t,0) = n\,\frac{\beta(u(t),v(t))\,u(t)\,v(t)}{1+\beta(u(t),v(t))\,h\,u(t)},$$

and the biologically natural terminal condition $b(t,\infty)=0$. The mature predator density is

$$v(t) = \int_\tau^\infty b(t,\alpha)\,d\alpha.$$

Solving (2.3) along characteristics yields $b(t,\tau) = b(t-\tau,0)\,e^{-\delta\tau}$ and hence

$$\begin{aligned} \frac{dv(t)}{dt} &= b(t,\tau) - m\,v(t) = b(t-\tau,0)\,e^{-\delta\tau} - m\,v(t) \\ &= n\,e^{-\delta\tau}\,\frac{\beta\big(u(t-\tau),v(t-\tau)\big)\,u(t-\tau)\,v(t-\tau)}{1+\beta\big(u(t-\tau),v(t-\tau)\big)\,h\,u(t-\tau)} - m\,v(t), \end{aligned}$$

where the diluted factor $e^{-\delta\tau}$ accounts for juvenile mortality during maturation, and

$$\beta\big(u(t-\tau),v(t-\tau)\big) = b_0 + \frac{a\,v(t-\tau)}{c\,u(t-\tau)+v(t-\tau)}.$$

Combining the prey equation from (2.1) with the above delayed predator equation gives

$$\begin{cases} \dfrac{du(t)}{dt} = ru(t)\left(1-\dfrac{u(t)}{K}\right) - \dfrac{\beta(u(t),v(t))\,u(t)\,v(t)}{1+\beta(u(t),v(t))\,h\,u(t)}, \\ \dfrac{dv(t)}{dt} = n\,e^{-\delta\tau}\,\dfrac{\beta\big(u(t-\tau),v(t-\tau)\big)\,u(t-\tau)\,v(t-\tau)}{1+\beta\big(u(t-\tau),v(t-\tau)\big)\,h\,u(t-\tau)} - m\,v(t), \end{cases} \tag{2.4}$$

subject to nonnegative continuous histories $(u(\theta),v(\theta))\in C([-\tau,0],\mathbb{R}^2_{\ge 0})$ with $u(0),v(0)>0$. In (2.4), $\tau>0$ is the fixed maturation delay, $\delta>0$ the juvenile mortality rate during $[0,\tau]$, and $\beta(\cdot,\cdot)$ is as in (2.2).

To reduce the number of parameters, we perform the nondimensionalization

$$u_1 = \frac{u}{K}, \qquad v_1 = \frac{v}{r}, \qquad t_1 = rt, \qquad \tau_1 = r\tau,$$

with the rescaled parameters

$$\tilde a = a, \qquad \tilde c = \frac{cK}{r}, \qquad \tilde h = hK, \qquad \tilde m = \frac{m}{r}, \qquad \tilde n = \frac{nK}{r}, \qquad \tilde\delta = \frac{\delta}{r}.$$

Dropping tildes and subscripts for notational simplicity (i.e., relabeling $(u_1,v_1,t_1,\tau_1)\mapsto(u,v,t,\tau)$), Eq. (2.1) can be written as

$$\begin{cases} \dfrac{du(t)}{dt} &= u(t)\big(1-u(t)\big) - \dfrac{\beta(u(t),v(t))\,u(t)\,v(t)}{1+\beta(u(t),v(t))\,h\,u(t)} \\ &=:\; f(u(t),v(t)) \;=\; u(t)\,f_1(u(t),v(t)), \\ \dfrac{dv(t)}{dt} &= n\,\dfrac{\beta(u(t),v(t))\,u(t)\,v(t)}{1+\beta(u(t),v(t))\,h\,u(t)} - m\,v(t) =:\; g(u(t),v(t)) \;=\; v(t)\,g_1(u(t),v(t)), \end{cases} \tag{2.5}$$

with

$$\beta(u(t),v(t)) \;=\; b_0 + \frac{a\,v(t)}{c\,u(t)+v(t)}.$$

Unless stated otherwise, all parameters in (2.5) are assumed to be positive.

In parallel, Eq. (2.4) becomes

$$\begin{cases} \dfrac{du(t)}{dt} = u(t)(1-u(t)) - \dfrac{\beta(u(t),v(t))\,u(t)\,v(t)}{1+\beta(u(t),v(t))\,h\,u(t)}, \\ \dfrac{dv(t)}{dt} = n\,e^{-\delta\tau}\,\dfrac{\beta\big(u(t-\tau),v(t-\tau)\big)\,u(t-\tau)\,v(t-\tau)}{1+\beta\big(u(t-\tau),v(t-\tau)\big)\,h\,u(t-\tau)} - m\,v(t), \end{cases} \tag{2.6}$$

## 3. Dynamics without maturation delay

### 3.1. Preliminaries

We first establish the positivity and boundedness of the solutions to the system (2.5), which are essential for biological realism and stability in simulations.

**Theorem 3.1.** *The solutions of system (2.5) are positive and uniformly bounded for all $t > 0$.*

**Proof.** The right-hand side of system (2.5) is continuous and locally Lipschitz on $\mathbb{R}^2_+$. By the existence and uniqueness theorems of solutions of ordinary differential equations, there exists a unique local solution on $[0, T)$ for any $T > 0$. Furthermore, since the system preserves nonnegativity, we have $u(t) > 0$ and $v(t) > 0$ for all $t \in [0, T)$. Then,

$$\begin{aligned}\frac{d}{dt}(nu(t) + v(t)) &= nu(t)(1 - u(t)) - mv(t)\\ &\le n(1 - u(t)) - mv(t)\\ &\le n - \min\{1, m\}(nu(t) + v(t)) \le n - \min\{1, m\}W(t).\end{aligned}$$

By Grönwall's inequality, it follows that $W(t) = nu(t) + v(t)$ is uniformly bounded on $[0, T)$. Therefore, $u(t)$ and $v(t)$ remain positive and bounded for all $t \in [0, T)$. As the solution does not blow up in finite time, it can be extended globally. Therefore, the solution exists uniquely for all $t > 0$ and is continuous with respect to initial conditions. □

The local stability behavior of system (2.5) near ecologically relevant equilibrium points is analyzed using linear stability analysis. The Jacobian matrix of the model (2.5) at the any equilibrium $E(u, v)$ is given by

$$J(E) = \begin{pmatrix} a_{10} & a_{01} \\ b_{10} & b_{01} \end{pmatrix}, \tag{3.1}$$

where

$$a_{10} = \frac{\partial f(u,v)}{\partial u} = 1 - 2u - A_1(u, v), \quad a_{01} = \frac{\partial f(u,v)}{\partial v} = -A_2(u, v) < 0,$$
$$b_{10} = \frac{\partial g(u,v)}{\partial u} = nA_1(u, v), \qquad b_{01} = \frac{\partial g(u,v)}{\partial v} = nA_2(u, v) - m,$$

with

$$A_1(u, v) = \frac{\left[\left(b_0 + \frac{av}{cu+v}\right) - \frac{acuv}{(cu+v)^2}\right]v}{\left[1 + \left(b_0 + \frac{av}{cu+v}\right)hu\right]^2},$$

$$A_2(u, v) = \frac{\frac{acu^2v}{(cu+v)^2} + \left(b_0 + \frac{av}{cu+v}\right)u + \left(b_0 + \frac{av}{cu+v}\right)^2 hu^2}{\left[1 + \left(b_0 + \frac{av}{cu+v}\right)hu\right]^2}.$$

The characteristic equation corresponding to the linearized system at $E$ is

$$\lambda^2 - \mathrm{Tr}(J(E))\lambda + \mathrm{Det}(J(E)) = 0, \tag{3.2}$$

where the trace and determinant of the Jacobian are given by

$$\mathrm{Tr}(J(E)) = 1 - m - 2u - A_1(u, v) + nA_2(u, v),$$

$$\mathrm{Det}(J(E)) = (1 - 2u - A_1(u, v))(nA_2(u, v) - m) + nA_1(u, v)A_2(u, v).$$

### 3.2. Equilibrium points and their stability

System (2.5) admits two boundary equilibria, $E_0(0, 0)$ and $E_1(1, 0)$, for any parameter values. The stability properties of these equilibria are summarized below.

**Theorem 3.2.** *System (2.5) has two boundary equilibria: $E_0(0, 0)$ and $E_1(1, 0)$. $E_0$ is always an unstable node. The stability of $E_1$ depends on the system parameters as follows:*

*(i) If $m < \frac{nb_0}{1 + b_0h}$ (i.e., $h < \frac{n}{m} - \frac{1}{b_0}$), then $E_1(1, 0)$ is a saddle.*

*(ii) If $m > \frac{nb_0}{1 + b_0h}$ (i.e., $h > \frac{n}{m} - \frac{1}{b_0}$), then $E_1(1, 0)$ is a stable node.*

*(iii) The equilibrium $E_1(1, 0)$ undergoes a transcritical bifurcation at*

$$h_{\mathrm{TC}} = \frac{n}{m} - \frac{1}{b_0},$$

*which satisfies the condition $m = \frac{nb_0}{1 + b_0h}$.*

**Proof.** We analyze the local stability of the system at two boundary equilibria $E_0(0, 0)$ and $E_1(1, 0)$.

We can firstly verify that a trivial equilibrium $E_0(0, 0)$ is always unstable given the Jacobian matrix for the model (2.5) at $E_0(0, 0)$ has two positive eigenvalue $\lambda = 1$ and $\lambda = -m$.

Next, the Jacobian matrix at $E_1(1, 0)$ is

$$J(E_1) = \begin{pmatrix} -1 & -\frac{b_0}{1 + b_0h} \\ 0 & -\left(m - \frac{nb_0}{1 + b_0h}\right) \end{pmatrix}.$$

The eigenvalues of $J(E_1)$ are $\lambda_1 = -1$, $\lambda_2 = -\left(m - \frac{nb_0}{1 + b_0h}\right)$. Thus, $E_1$ is locally asymptotically stable if $\lambda_2 < 0$, i.e., when $m > \frac{nb_0}{1 + b_0h}$, and is a saddle if $\lambda_2 > 0$. Therefore, $E_1$ loses stability via a transcritical bifurcation at the critical threshold $h_{\mathrm{TC}} = \frac{n}{m} - \frac{1}{b_0}$, which is equivalent to $m = \frac{nb_0}{1 + b_0h}$. Specifically, $E_1$ is stable for $h > h_{\mathrm{TC}}$, while it becomes unstable for $h < h_{\mathrm{TC}}$. □

Theorem 3.2 shows that if the handling time $h$ is too long or the death rate $m$ is too high, the predator cannot persist, and the system converges to the prey-only equilibrium $E_1(1, 0)$.

In the following, we investigate the number and stability of positive equilibrium points $E(u, v)$ for system (2.5). By simultaneously solving $f(u, v) = 0$ and $g(u, v) = 0$ and eliminating the variable $v$, we derive a quadratic equation in $u$:

$$F_0(u) = \alpha_0u^2 - \beta_0u + \gamma_0 = 0, \ (0 < u < 1), \tag{3.3}$$

where

$$\alpha_0 = (n - mh)(b_0 + a)n, \quad \beta_0 = mn + (n - mh)[b_0mc + n(b_0 + a)],$$
$$\gamma_0 = m(mc + n) > 0.$$

Using the relationship between the roots and coefficients of a quadratic equation, we obtain $v = \frac{(n-mh)b_0cu^2 - mcu}{m-(n-mh)(b_0+a)} < 0$ when $n \le mh$. Hence, $n > mh$ is the necessary condition for the existence of positive equilibria from Eq. (3.3).

From the quadratic formula, the discriminant $\Delta_0$ of Eq. (3.3) is given by

$$\begin{aligned}\Delta_0 &= \beta_0^2 - 4\alpha_0\gamma_0\\ &= \left\{mn + (n - mh)\left[b_0mc + n(b_0 + a)\right]\right\}^2 - 4mn(n - mh)(b_0 + a)(mc + n).\end{aligned}$$

Under the condition $h < \frac{n}{m}$, we have $F_0(0) = m(mc + n) > 0$ and $F_0(1) = mc(m - (n - mh)b_0)$. Based on this, we can conclude:

(1) If $F_0(1) > 0$, then:
- Eq. (3.3) has two distinct positive roots if $\Delta_0 > 0$;
- It has a double positive root if $\Delta_0 = 0$;
- It has no positive root if $\Delta_0 < 0$.

(2) If $F_0(1) < 0$, then Eq. (3.3) has exactly one positive root.

Next, we analyze the number of positive roots of (3.3) by treating $h$ as a bifurcation parameter. Rearranging $\Delta_0$ yields a quadratic in $h$:

$$\mathbf{F}_0(h) = P_{0,h}h^2 - Q_{0,h}h + R_{0,h} = 0, \tag{3.4}$$

with

$$P_{0,h} = m^2\left[b_0mc + n(b_0+a)\right]^2 > 0,$$
$$Q_{0,h} = 2mn\left[b_0mc + n(b_0+a)\right]^2 + 2m^2n\left[b_0mc + n(b_0+a)\right] - 4m^2n(b_0+a)(mc+n),$$
$$R_{0,h} = m^2n^2 + 2mn^2\left[b_0mc + n(b_0+a)\right] + n^2\left[b_0mc + n(b_0+a)\right]^2 - 4mn^2(b_0+a)(mc+n).$$

The roots of Eq. (3.4), which correspond to bifurcation thresholds in $h$, are given by

$$h_1 = \frac{Q_{0,h} - \sqrt{\Delta_{2,h}}}{2P_{0,h}}, \quad h_2 = \frac{Q_{0,h} + \sqrt{\Delta_{2,h}}}{2P_{0,h}}, \quad \Delta_{0,h} = Q_{0,h}^2 - 4P_{0,h}R_{0,h}.$$

Based on the nature of the roots of Eq. (3.4), the following lemma is given.

**Lemma 3.1.** *Given $h < \frac{n}{m}$, the number of positive roots of Eq. (3.4) is determined as follows:*

*(i) If $\Delta_{0,h} > 0$, $R_{0,h} > 0$, and $0 < \frac{Q_{0,h}}{2P_{0,h}} < \frac{n}{m}$, then Eq. (3.4) admits two positive roots $h_1$ and $h_2$, with $h_1 < h_2$.*

*(ii) If $\Delta_{0,h} = 0$, $R_{0,h} > 0$, and $0 < \frac{Q_{0,h}}{2P_{0,h}} < \frac{n}{m}$, then Eq. (3.4) admits one positive root $h_1 = h_2 = \frac{Q_{0,h}}{2P_{0,h}}$.*

*(iii) If $\mathbf{F}_0(0) < 0$, then Eq. (3.4) has one positive root $h_2$.*

In fact, due to the constraint $u \in (0,1)$, the larger root $h_2$ does not correspond to a biologically feasible equilibrium of system (2.5), and hence may be discarded in applications. Define

$$h(u) = \frac{n}{m} - \frac{1}{uG(u)}, \qquad G(u) = b_0 + \frac{an(1-u)}{mc + n(1-u)} > 0, \quad u \in (0,1).$$

We note that

$$G(u_{**}) = 0, \qquad u_{**} = 1 + \frac{b_0mc}{n(b_0+a)} > 1,$$

and

$$h'(u) = \frac{G(u) + uG'(u)}{(uG(u))^2}, \qquad G'(u) = -\frac{amnc}{(mc + n(1-u))^2} < 0.$$

There exists $u_0 \in (0,1)$ such that $h'(u_0) = 0$. Furthermore, using limit theory and monotonicity, we obtain:

$$\lim_{u\to 0^+} h(u) = -\infty, \qquad \lim_{u\to 1^-} h(u) = \frac{n}{m} - \frac{1}{b_0}, \qquad \lim_{u\to u_{**}} h(u) = -\infty,$$
$$\lim_{u\to u_{**}^+} h(u) = +\infty, \qquad \lim_{u\to+\infty} h(u) = \frac{n}{m}.$$

It is trivial to verify that $h_1$ satisfies the required conditions, while $h_2$ does not exist due to biological constraints. Next, we analyze the number of positive equilibria of system (2.5). Hence, we obtain the following result.

**Lemma 3.2.** *The system (2.5) has at most two positive equilibria. Moreover,*

*(i) If $\frac{n}{m} - \frac{1}{b_0} < h < \frac{n}{m}$, then:*

*(i1) System (2.5) has no positive equilibria when $h_1 < h$;*

*(i2) System (2.5) has two positive equilibria $E_2(u_2,v_2)$ and $E_3(u_3,v_3)$ when $\frac{n}{m} - \frac{1}{b_0} < h < h_1$, where*

$$u_2 = \frac{\beta_0 - \sqrt{\beta_0^2 - 4\alpha_0\gamma_0}}{2\alpha_0}, \quad v_2 = \frac{nu_2(1-u_2)}{m};$$
$$u_3 = \frac{\beta_0 + \sqrt{\beta_0^2 - 4\alpha_0\gamma_0}}{2\alpha_0}, \quad v_3 = \frac{nu_3(1-u_3)}{m}.$$

*(i3) System (2.5) has a unique positive (degenerate) equilibrium $E_*(u_*,v_*)$ when $h = h_1$, where*

$$u_* = \frac{\beta_0}{2\alpha_0}, \quad v_* = \frac{nu_*(1-u_*)}{m} = \frac{n\beta_0(2\alpha_0 - \beta_0)}{4m\alpha_0^2},$$

*(i4) In all other cases, system (2.5) has no positive equilibria.*

*(ii) If $0 < h < \frac{n}{m} - \frac{1}{b_0}$, then system (2.5) has one positive equilibrium $E_2(u_2,v_2)$, where $u_2$ and $v_2$ are given above.*

**Proof.** The condition $h < \frac{n}{m}$ is necessary for ensuring $v = \frac{(n-mh)b_0cu^2 - mcu}{m - (n-mh)(b_0+a)} > 0$. Therefore, our analysis assumes that $h < \frac{n}{m}$ throughout. Given $\alpha_0 > 0$, $\gamma_0 > 0$, and $\beta_0 > 0$, we have: $F_0(0) = \gamma_0 > 0$, and $u_* = \frac{\beta_0}{2\alpha_0} > 0$. Additionally, $F_0(1) = mc\left(m - (n-mh)b_0\right)$, and we have

- If $F_0(1) > 0$, which occurs when $h > \frac{n}{m} - \frac{1}{b_0}$.
  - If $\Delta_0 < 0$ (i.e., $h > h_1$), then Eq. (3.3) has no positive root.
  - If $\Delta_0 = 0$ (i.e., $h = h_1$), then there is a unique double root, hence a degenerate positive equilibrium.
  - If $\Delta_0 > 0$ and $\frac{n}{m} - \frac{1}{b_0} < h < h_1$, then two distinct positive equilibria exist.
- If $F_0(1) < 0$, which corresponds to $h < \frac{n}{m} - \frac{1}{b_0}$, then Eq. (3.3) always has one positive root.

Hence, system (2.5) has at most two positive equilibria, and the conditions under which they exist are established. □

Through the sign relationship between the trace $\mathrm{Tr}(J(E))$ and the determinant $\mathrm{Det}(J(E))$ of the Jacobian matrix $J(E)$, and together with the results in [27], the stability and local phase portrait characteristics of the positive equilibrium point $E(u,v)$ of system (2.5) can be analyzed.

**Theorem 3.3.** *Assume $h < \frac{n}{m}$, then the dynamical behaviour of the positive equilibrium $E(u,v)$ of system (2.5) is as follows:*

*(i) If system (2.5) admits a unique positive equilibrium $E_2(u_2,v_2)$, then:*
- *$E_2$ is a stable focus (or node) if $\mathrm{Tr}\left(J(E_2)\right) < 0$;*
- *$E_2$ is an unstable focus (or node) if $\mathrm{Tr}\left(J(E_2)\right) > 0$;*
- *$E_2$ is a weak focus (or a center) if $\mathrm{Tr}\left(J(E_2)\right) = 0$.*

*(ii) If system (2.5) admits two positive equilibria $E_2(u_2,v_2)$ and $E_3(u_3,v_3)$ with $u_2 < u_3$, then $E_3$ is always a saddle point, and:*
- *$E_2$ is a stable focus (or node) if $\mathrm{Tr}\left(J(E_2)\right) < 0$;*
- *$E_2$ is an unstable focus (or node) if $\mathrm{Tr}\left(J(E_2)\right) > 0$;*
- *$E_2$ is a weak focus (or a center) if $\mathrm{Tr}\left(J(E_2)\right) = 0$.*

*The phase portraits are shown in Fig. 1.*

**Proof.** For the sake of clarity, we denote the positive equilibrium of system (2.5) as $E^*(u^*,v^*)$. Combining the steady-state conditions $f(u^*,v^*) = 0$ and $g(u^*,v^*) = 0$, we obtain:

$$v^* = \frac{n}{m}u^*(1-u^*). \tag{3.5}$$

The derivative of the implicit function defined by $f(u,v(u)) = 0$ with respect to $u$ is

$$\left.\frac{dv(u)}{du}\right|_{u=u^*} = -\left.\frac{\partial f(u,v)/\partial u}{\partial f(u,v)/\partial v}\right|_{u=u^*}.$$

Substituting (3.5) into $g(u^*,v^*) = 0$ yields

$$H(u^*) = -\frac{nu^*(1-u^*)}{m[mc + n(1-u^*)](1 + b_0\ hu^*) + mnhau^*(1-u^*)}F(u^*) = 0,$$

where $F(u)$ is defined in (3.3). Differentiating $H(u)$ with respect to $u$ gives

$$\left[\frac{\partial g(u,v(u))}{\partial v}\frac{dv(u)}{du} + \frac{\partial g(u,v(u))}{\partial u}\right]_{u=u^*} = \left.\frac{dF(u)}{du}\right|_{u=u^*}.$$

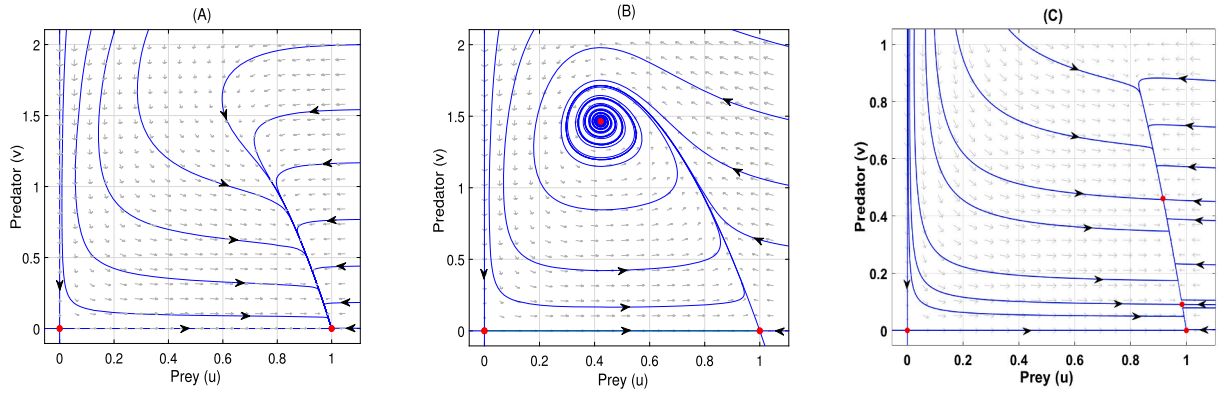


**Fig. 1.** Phase portraits of system (2.5) showing the changes in number of positive equilibria under varying $h$. (A) $h = 5.3 > 5.04349$; (B) $h = 4 < 5$; (C) $5 < h = 5.03 < 5.04349$.

Therefore, we have

$$\begin{aligned}&\frac{dF(u)}{du}|_{u=u^*}\frac{\partial f(u,v)}{\partial v}|_{u=u^*}\\&\quad=-\frac{\partial g(u,v(u))}{\partial v}|_{u=u^*}\frac{\partial f(u,v)}{\partial u}|_{u=u^*}\\&\qquad+\frac{\partial g(u,v(u))}{\partial u}|_{u=u^*}\frac{\partial f(u,v)}{\partial v}|_{u=u^*}=-\mathrm{Det}(J(E^*)).\end{aligned}$$

We can further see that

$$\begin{aligned}\mathrm{Det}(J(E^*))&=-\frac{dF(u)}{du}|_{u=u^*}\frac{\partial f(u,v)}{\partial v}|_{u=u^*}\\&=-\frac{nu^*(1-u^*)A_2}{m[mc+n(1-u^*)]\left(1+b_0hu^*\right)+mnhau^*(1-u^*)}F'\left(u^*\right).\end{aligned}$$

Thus, with the characteristic Eq. (3.2), the sign of $\mathrm{Det}(J(E^*))$ is the opposite of the sign of $F'(u^*)$:

$$\mathrm{sign}\left(\mathrm{Det}\left(J\left(E^*\right)\right)\right)=-\mathrm{sign}\left(F'\left(u^*\right)\right).$$

Since $\mathrm{Det}(J(E_3)) < 0$, the equilibrium $E_3$ is a saddle. Conversely, $\mathrm{Det}(J(E_2)) > 0$, so the nature of $E_2$ depends on $\mathrm{Tr}(J(E_2))$ as stated in the theorem. □

When there is a single coexistence state, small disturbances either decay and the system returns to coexistence, or grow and drive the system away from it. When two coexistence equilibria exist, one acts as an unstable threshold that separates long-term outcomes: initial conditions on one side approach stable coexistence, whereas those on the other side may lead to predator extinction. Theorem 3.3 shows that predator persistence is threshold-dependent, implying that successful biological control requires sufficiently large predator releases and favorable initial conditions to cross this threshold.

Fixing the parameters as $b_0 = 1$, $a = 0.2$, $c = 0.3$, $m = 0.5$, and $n = 3$, we obtain the following results:

(1) System (2.5) has no coexistence equilibrium when $h = 5.3 > 5.04349$. The predator-free equilibrium $E_1(1,0)$ is a stable node; see Fig. 1(A).
(2) System (2.5) has one single coexistence equilibrium $E_2(0.4223, 1.4638)$, which is a stable focus, when $h = 4 < 5$. Specifically, $\mathrm{Tr}(J(E_2)) = -0.0327 < 0$ and $\mathrm{Det}(J(E_2)) = 0.0954 > 0$. The predator-free point $E_1(1,0)$ becomes a saddle; see Fig. 1(B).
(3) System (2.5) admits two coexistence equilibria when $5 < h = 5.03 < 5.04349$:
   - $E_2(0.9161, 0.4610)$ is a stable node with $\mathrm{Tr}(J(E_2)) = -0.8419 < 0$ and $\mathrm{Det}(J(E_2)) = 0.0037 > 0$;
   - $E_3(0.9846, 0.0908)$ is an unstable node with $\mathrm{Tr}(J(E_3)) = -0.9689 < 0$ and $\mathrm{Det}(J(E_3)) = -0.0015 < 0$.

   The predator-free equilibrium $E_1(1,0)$ remains a stable node; see Fig. 1(C).

According to Lemma 3.2, the number of equilibria in system (2.5) is determined by the parameter $h$. We now analyze the unique positive equilibrium $E_*(u_*, v_*)$ when it exists.

**Theorem 3.4.** *Suppose $h = h_1$, the system (2.5) has a unique, degenerate positive equilibrium $E_*(u_*, v_*)$. Moreover,*

*(i) If $m \neq 1 - 2u_* - A_1(u_*, v_*) + nA_2(u_*, v_*)$, then $E_*$ is a saddle-node. Furthermore:*
   - *$E_*$ is attracting if $m > 1 - 2u_* - A_1(u_*, v_*) + nA_2(u_*, v_*)$;*
   - *$E_*$ is repelling if $m < 1 - 2u_* - A_1(u_*, v_*) + nA_2(u_*, v_*)$.*

   *Phase portraits are illustrated in Fig. 2(A)-(B).*
*(ii) If $m = 1 - 2u_* - A_1(u_*, v_*) + nA_2(u_*, v_*)$, then $E_*(u_*, v_*)$ is a cusp. The behavior near $E_*$ is further characterized as:*
   *(ii1) If $\mathcal{D} \neq 0$ and $\mathcal{E} \neq 0$, then $E_*$ is a cusp of codimension 2 (i.e., a Bogdanov–Takens singularity). The phase portrait is shown in Fig. 2(C).*
   *(ii2) If $\mathcal{D} \neq 0$ and $\mathcal{E} = 0$, then $E_*$ is a nilpotent cusp of codimension at least 3.*
   *(ii3) If $\mathcal{D} = 0$, then $E_*$ is a nilpotent saddle (or focus, or elliptic singularity) of codimension at least 3.*

**Proof.** By computing the determinant and trace of the Jacobian matrix of system (2.5) at the equilibrium $E_*(u_*, v_*)$, we have

$$\mathrm{Det}\left(J\left(E_*\right)\right)=0,\quad\text{and}\quad\mathrm{Tr}\left(J\left(E_*\right)\right)=1-m-2u_*-A_1(u_*,v_*)+nA_2(u_*,v_*).$$

If $\mathrm{Tr}(J(E_*)) = 0$, i.e. $m = 1 - 2u_* - A_1(u_*, v_*) + nA_2(u_*, v_*)$, both eigenvalues of the Jacobian matrix of system (2.5) are zeros. If one eigenvalue is zero and the other is non-zero, then the nature of $E_*(u_*, v_*)$ can be analyzed using the criteria given in Zhang [28].

We now perform the coordinate transformation $u_1 = u - u_*$ and $v_1 = v - v_*$, moving the equilibrium $E_*(u_*, v_*)$ to $(0,0)$. Applying this transformation to system (2.5) and expanding it into a Taylor series up to the second-order terms yields

$$\begin{cases}\dfrac{du_1}{dt}=\displaystyle\sum_{i+j=1}^{2}a_{ij}u_1^iv_1^j+O_1\left(|(u_1,v_1)|^2\right),\\[2ex]\dfrac{dv_1}{dt}=\displaystyle\sum_{i+j=1}^{2}b_{ij}u_1^iv_1^j+O_2\left(|(u_1,v_1)|^2\right),\end{cases}\tag{3.6}$$

where $a_{ij}$ and $b_{ij}$ $(i, j = 0, 1, 2, i + j \leq 2)$ are the coefficients in the Taylor expansions of $f(u, v)$ and $g(u, v)$ at $E_*(u_*, v_*)$, and $O_k\left(|(u_1, v_1)|^4\right)$ $(k = 1, 2)$ represent higher-order terms.

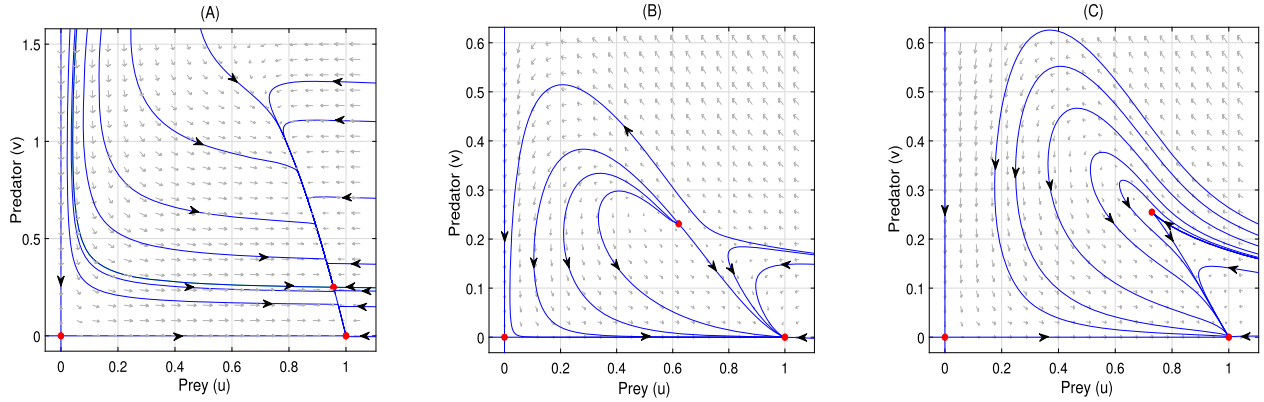


**Fig. 2.** Phase portraits of system (2.5) with a single equilibrium under various parameter sets. (A) $E_*(0.9565, 0.2499)$ (B)$E_*(0.6211, 0.2310)$ (C) $E_*(0.7288, 0.2549)$.

Furthermore, we apply a linear transformation $u = u_1$, $v = a_{10}u_1 + a_{01}v_1$, and obtain

$$\begin{cases} \dfrac{du}{dt} = v + O\big(|(u_1, v_1)|^2\big), \\ \dfrac{dv}{dt} = \mathcal{D}u^2 + \mathcal{E}uv + O\big(|(u_1, v_1)|^2\big), \end{cases} \tag{3.7}$$

with

$$\mathcal{D} = \frac{a_{10}a_{20}a_{01}^2 - a_{01}a_{11}a_{10}^2 + a_{02}a_{10}^3 + b_{20}a_{10}^2 - b_{11}a_{10}a_{01} + a_{10}^2 b_{02}}{a_{01}^2},$$

$$\mathcal{E} = -\frac{a_{10}a_{01}a_{11} + 4a_{10}^2 a_{02} + 2a_{10}b_{20} + 2a_{10}b_{02} - a_{10}b_{11} - 2a_{20}a_{01}^2}{a_{01}^2}.$$

The dynamical behaviour near the $E_*(u_*, v_*)$ can be determined based on both the signs and values of $\mathcal{D}$ and $\mathcal{E}$, as already discussed in [27,29,30]. □

The phase portraits of system (2.5) with a single equilibrium are illustrated through three numerical simulations:

(1) $E_*(0.9565, 0.2499)$ is an attracting saddle-node, obtained under the parameter values $b_0 = 1$, $a = 0.2$, $c = 0.3$, $m = 0.5$, $n = 3$, and $h = 5.04352036$, with $\mathrm{Tr}(J(E_*)) = -0.9159 < 0$; see Fig. 2(A).
(2) $E_*(0.6211, 0.2310)$ is a repelling saddle-node, obtained under the parameter values $b_0 = 1$, $c = 2.5$, $n = 3$, $h = 0.5$, $a = 18.0834956$, and $m = 3.0558127$, with $\mathrm{Tr}(J(E_*)) = 0.6 > 0$; see Fig. 2(B).
(3) $E_*(0.7288, 0.2549)$ is a cusp, obtained under the parameter values $b_0 = 1$, $c = 2.5$, $n = 3.1812886$, $h = 0.5$, $a = 6$, and $m = 2.4659045$, where $\mathrm{Tr}(J(E_*)) = 0$; see Fig. 2(C).

### 3.3. Local bifurcation

#### 3.3.1. Transcritical bifurcation

**Theorem 3.5.** *System (2.5) undergoes a transcritical bifurcation at the predator-free equilibrium $E_1(1, 0)$ as the parameter $h$ (or $m$) crosses the critical value critical value $h_{TC} = \frac{n}{m} - \frac{1}{b_0}$ or $m_{TC} = \frac{nb_0}{1+hb_0}$.*

**Proof.** The Jacobian matrix $J(E_1)$ has a simple zero eigenvalue at $h = \frac{n}{m} - \frac{1}{b_0}$. Let $M$ and $N$ denote the right and left eigenvectors of $J(E_1)$ and $J^T(E_1)$, respectively, corresponding to the zero eigenvalue. Then, $M = \left[1 \ -\frac{(1+b_0h)}{b_0}\right]^T$ and $N = [0\ 1]^T$. We define $H(u, v) = (f(u, v), g(u, v))$ and compute the relevant transversality and non-degeneracy conditions:

$$N^T H_h(E_1; h = h_{TC}) = 0,$$

$$N^T DFH_h(E_1; h = h_{TC})(M) = -2nb_0(1 + b_0\ h)^2 \neq 0,$$

$$N^T D^2 H(E_1; h = h_{TC})(M, M) = \frac{\partial^2 g}{\partial u^2} - 2\frac{\partial^2 g}{\partial u \partial v} \cdot \frac{1 + b_0 h}{b_0} + \frac{\partial^2 g}{\partial v^2} \cdot \frac{(1 + b_0\ h)^2}{b_0^2}$$

$$= \frac{2na(1 + b_0\ h)^2}{b_0^2 c}\big[1 + b_0 h(2 + h)\big] \neq 0.$$

Hence, all the required conditions for a codimension-one transcritical bifurcation are satisfied. By Sotomayor's theorem, system (2.5) undergoes a transcritical bifurcation at $E_1(1, 0)$ when $h = h_{\mathrm{TC}}$. □

#### 3.3.2. Saddle-node bifurcation

**Theorem 3.6.** *System (2.5) undergoes a saddle-node bifurcation at the coexistence equilibrium point $E_*(u_*, v_*)$ as the parameter $h$ crosses a critical value $h = h_{\mathrm{SN}}$. At this threshold, the equation $F(u) = 0$ has a double root denoted by $u_*$.*

**Proof.** Since the polynomial equation $F(u) = 0$ has a double root $u_*$ at $h = h_{\mathrm{SN}}$, we have

$$F\big(u_*, h_{SN}\big) = 0, \quad F'\big(u_*, h_{SN}\big) = 0, \quad \text{but } F''\big(u_*, h_{SN}\big) = m(mc + n) \neq 0.$$

This indicates that the two non-trivial nullclines $f_1(u, v) = 0$ and $g_1(u, v) = 0$ intersect at $(u_*, v_*)$ when $h = h_{\mathrm{SN}}$:

$$f_1\big(u_*, v_*\big) = 0 \quad \text{and} \quad g_1\big(u_*, v_*\big) = 0 \quad \text{when } h = h_{SN}.$$

By the Implicit Function Theorem, we obtain

$$\frac{\partial f_1}{\partial u}\frac{\partial g_1}{\partial v}\bigg|_{(E_*, h_{SN})} = \frac{\partial f_1}{\partial v}\frac{\partial g_1}{\partial u}\bigg|_{(E_*, h_{SN})}.$$

On the other hand, for $h = h_{\mathrm{SN}}$, the Jacobian matrix $J(E_*)$ is given by

$$J(E_*) = \begin{pmatrix} f_u & f_v \\ g_u & g_v \end{pmatrix}_{(E_*, h_{SN})} = \begin{pmatrix} uf_{1u} & uf_{1v} \\ vg_{1u} & vg_{1v} \end{pmatrix}_{(E_*, h_{SN})},$$

which implies

$$\mathrm{Det}(J(E_*)) = \left[uv\left(\frac{\partial f_1}{\partial u}\frac{\partial g_1}{\partial v} - \frac{\partial f_1}{\partial v}\frac{\partial g_1}{\partial u}\right)\right]_{E_*} = 0.$$

Therefore, Jacobian matrix $J(E_*)$ has a zero eigenvalue, ensuring the necessary condition for a saddle-node bifurcation.

Let $M$ and $N$ be eigenvectors of the Jacobian matrices $J\big(E_*\big)$ and $J^T\big(E_*\big)$ corresponding to the simple zero eigenvalue, then we obtain

$$M = \begin{bmatrix} 1 \\ -\dfrac{f_{1u}(u_*, v_*)}{f_{1v}(u_*, v_*)} \end{bmatrix}, \quad N = \begin{bmatrix} 1 \\ -\dfrac{u_*}{v_*}\dfrac{f_{1u}(u_*, v_*)}{g_{1v}(u_*, v_*)} \end{bmatrix}.$$

We now verify the transversality conditions:

$$N^T H_h(E_*; h = h_{SN})$$

$$= -\left(1 + n\frac{u_*}{v_*}\frac{f_{1u}(u_*, v_*)}{g_{1v}(u_*, v_*)}\right)\frac{\left(b_0 + \dfrac{av_*}{cu_* + v_*}\right)u_*^2 v_*}{\left[1 + \left(b_0 + \dfrac{av_*}{cu_* + v_*}\right)hu_*\right]^2} \neq 0,$$

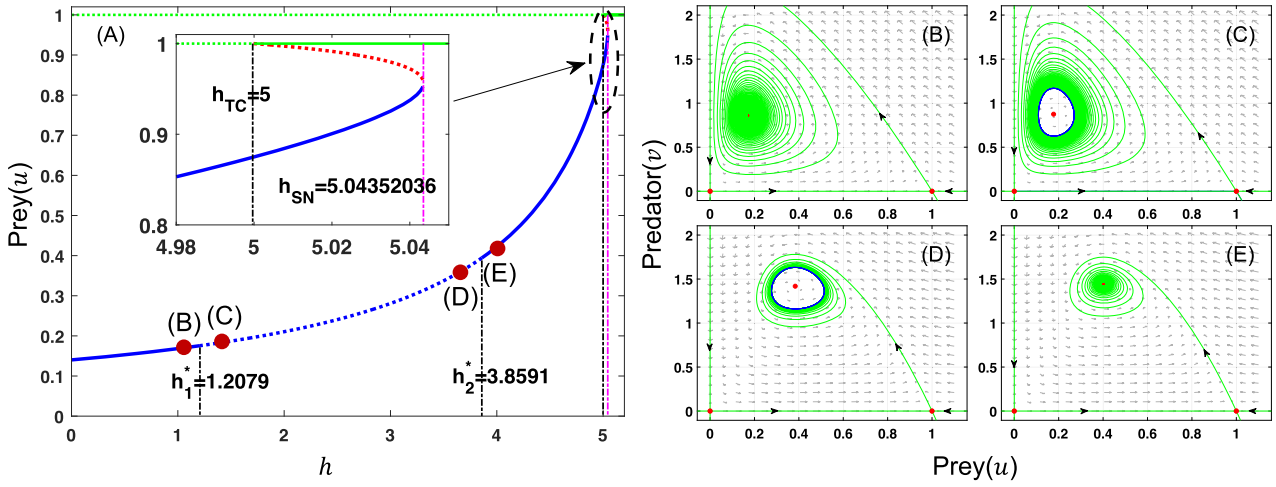


**Fig. 3.** (A) One-parameter bifurcation diagram of system (2.5) with $b_0 = 1$, $a = 0.2$, $c = 0.3$, $m = 0.5$, and $n = 3$. A transcritical bifurcation occurs at $h_{TC} = 5$, and a saddle-node bifurcation at $h_{SN} = 5.04352036$. The blue curve indicates $E_2$, and dashed part mark Hopf bifurcations bounded by $h_1^* = 1.2079$ and $h_2^* = 3.8591$. (B)-(E) Phase portraits for parameter values indicated in panel (A): (B) $h = 1.15 \in (0, h_1^*)$, (C) $h = 1.25 \in (h_1^*, h_2^*)$, (D) $h = 3.8 \in (h_1^*, h_2^*)$, (E) $h = 3.9 \in (h_2^*, h_{SN})$.

and the non-degeneracy conditions:

$$
\begin{aligned}
&N^T D^2 H\left(E_*; h = h_{SN}\right)(M, M) \\
&= f_{1uu}(u_*, v_*) + \frac{f_{1u}(u_*, v_*)}{f_{1v}(u_*, v_*)}\left(\frac{f_{1u}(u_*, v_*)}{f_{1v}(u_*, v_*)} f_{1vv}(u_*, v_*) - 2 f_{1uv}(u_*, v_*)\right) \\
&\quad - g_{1uu}(u_*, v_*)\frac{u_*}{v_*}\frac{f_{1u}(u_*, v_*)}{g_{1u}(u_*, v_*)} \\
&\quad - \frac{f_{1u}^2(u_*, v_*) u_*}{f_{1v}(u_*, v_*) g_{1u}(u_*, v_*) v_*}\left(\frac{f_{1u}(u_*, v_*)}{f_{1v}(u_*, v_*)} g_{1vv}(u_*, v_*) - 2 g_{1uv}(u_*, v_*)\right) \\
&\quad \neq 0.
\end{aligned}
$$

Since both conditions are satisfied, by Sotomayor's theorem, system (2.5) undergoes a saddle-node bifurcation at $E_*$ as $h$ passes through $h_{\mathrm{SN}}$. □

### 3.3.3. *Hopf bifurcation and limit cycle around the interior equilibrium* $E_2(u_2, v_2)$

According to Theorem 3.3, if the Jacobian matrix $J\left(E_2\right)$ satisfies $\mathrm{Tr}(J(E_2)) = 0$ and $\mathrm{Det}(J(E_2)) > 0$, then system (2.5) undergoes a Hopf bifurcation at $E_2$.

Assume that the corresponding determinant of the Jacobian matrix evaluated at $E_2(u_2, v_2)$ for the parametric value of $h = h_{HB}$. Then the corresponding characteristic equation will have two purely imaginary eigenvalues $\pm i\omega_0$, where

$$\omega_0 = \sqrt{\mathrm{Det}(J(E_2))|_{h=h_{HB}}}.$$

Let $\lambda = \beta(h) \pm i\omega(h)$ denote the eigenvalues of the characteristic equation (3.2). Then

$$\beta(h) = -\frac{1}{2}\mathrm{Tr}(J(E_2)), \quad \omega(h) = \frac{1}{2}\sqrt{\mathrm{Tr}(J(E_2))^2 - 4\,\mathrm{Det}(J(E_2))}.$$

Hence,

$$
\begin{aligned}
&\beta\left(h_{HB}\right) = -\frac{1}{2}\mathrm{Tr}(J(E_2))|_{h=h_{HB}}, \quad \frac{d\beta(h)}{dh}|_{h=h_{HB}} = -\frac{1}{2}\frac{d(\mathrm{Tr}(J(E_2)))}{dh}|_{h=h_{HB}} \\
&\quad \neq 0.
\end{aligned}
$$

Therefore, the transversality condition is satisfied and the system (2.5) undergoes a Hopf bifurcation at the positive equilibrium $E_2(u_2, v_2)$ for the critical parameter value $h = h_{HB}$.

To verify the existence of a stable periodic solution, we conduct numerical simulations using parameter values $b_0 = 1$, $a = 0.2$, $c = 0.3$, $m = 0.5$, and $n = 3$. Two critical Hopf bifurcation values are obtained: $h_1^* = 1.2079$ and $h_2^* = 3.8591$ (see Fig. 3(A)).

(1) At critical value $h_{HB} = h_1^* = 1.2079$, the first Lyapunov coefficient is $L = -0.03639 < 0$, indicating a supercritical Hopf bifurcation. $E_2(0.1735, 0.8603)$ of system (2.5) is asymptotically stable for $h = 1.15 < h_1^*$ (see Fig. 3(B)), and there exists a stable limit cycle around $E_2(0.1771, 0.8745)$ for $h = 1.25 > h_1^*$ (see Fig. 3(C)).

(2) At critical value $h_{HB} = h_2^* = 3.8591$, the first Lyapunov coefficient is $L = -0.03983 < 0$, again indicating a supercritical Hopf bifurcation. There exists a stable limit cycle around $E_2(0.3836, 1.4187)$ for $h = 3.8 < h_2^*$ (see Fig. 3(D)), and the $E_2(0.4020, 1.4424)$ of system (2.5) is asymptotically stable for $h = 3.9 > h_2^*$ (see Fig. 3(E)).

Fig. 3 shows how the handling time $h$ shapes the predator-prey dynamics. As $h$ increases, the predator's feeding efficiency decreases because a larger fraction of time is spent processing captured prey rather than searching for the next ones. This reduced efficiency introduces a substantial delay in the predator's response to changes in prey density. Hence predation pressure cannot increase immediately to track prey population growth, allowing the prey to reach relatively high densities. The elevated prey abundance subsequently provides sufficient resources to support predator reproduction through trophic conversion, leading to a delayed increase in predator density. However, as predation pressure relaxes, the remaining prey re-enter a growth phase, thereby reinitiating the cycle. When $h$ becomes sufficiently large, predation efficiency is severely diminished, and the predator can no longer compensate for its mortality through prey consumption. Under these conditions, predator persistence is no longer possible, and the predator population goes extinct. The system then reduces to a single-species dynamical system in which the prey population evolves independently of predation.

Recall that in model (2.5), the attack rate is no longer treated as a fixed parameter but a variable dynamically regulated by the parameters $a$, $b_0$, and $c$, as presented in (2.5). Specifically, $b_0$ represents the minimum attack rate, corresponding to the baseline level of attack rate when the consumer is in an extremely shy state. $a$ denotes the maximum possible increment in attack rate, capturing the enhancement in predation intensity associated with extremely bold behavior. Lastly, $c$ is the half-saturation constant governing the attack-rate increment based on boldness. A smaller $c$ indicates that even modest increases in boldness lead to substantial increases in the attack rate, whereas a larger $c$ corresponds to a weaker effect on predation.

To numerically verify the existence of a stable periodic solution in system (2.5), we fix the parameters $b_0 = 1$ and $h = 1$, and consider variations in a single bifurcation parameter while keeping the other three

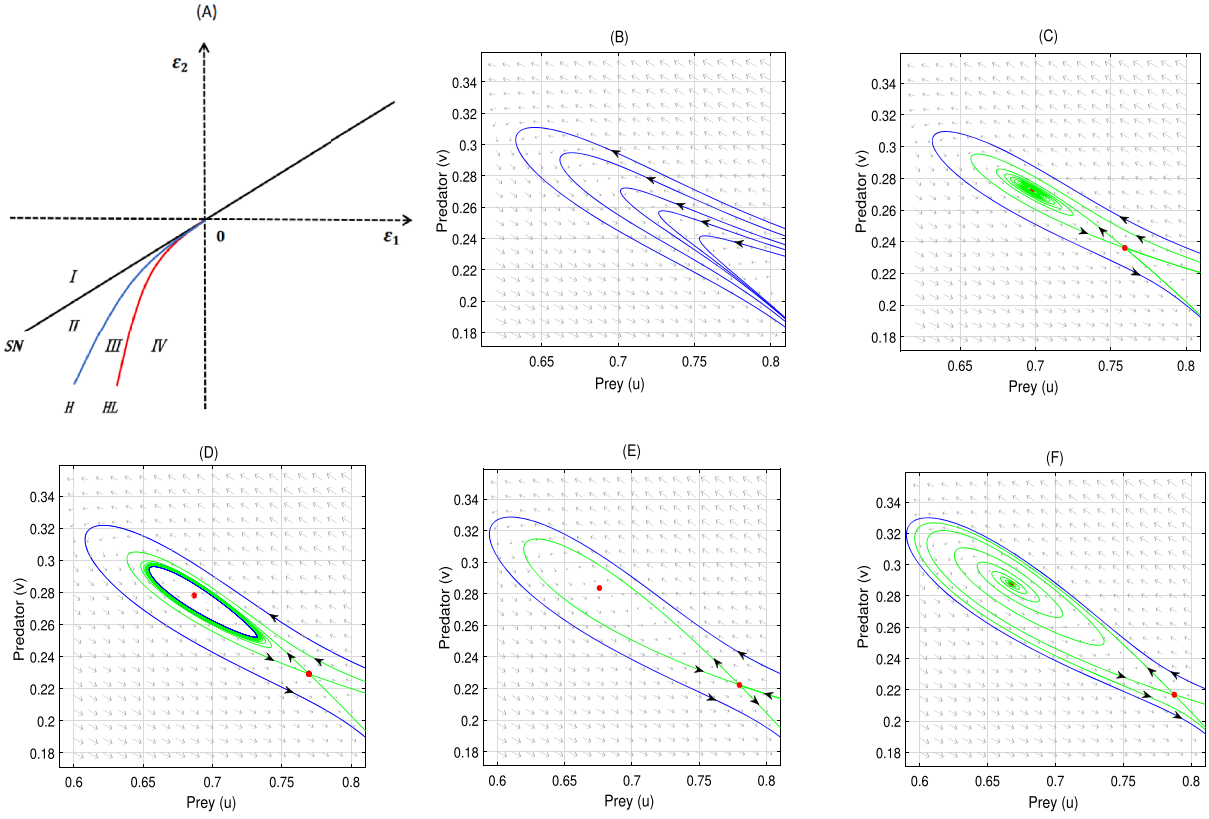


**Fig. 4.** (A)Attracting Bogdanov-Takens bifurcation diagram of system (2.5) with $b_0 = 1, h = 0.5, a = 6, c = 2.5, n_* = 3.1812886, m_* = 2.4659045$. (B)-(D)Phase diagrams of system (2.5) for different values of $(\varepsilon_1, \varepsilon_2)$ under fixed parameters: $b_0 = 1, h = 0.5, a = 6, c = 2.5$.

fixed. The results of Hopf bifurcation analysis under different parameter choices are summarized as follows:

(1) The individual boldness parameter $a$ itself is influenced by multiple factors such as prey density, predator hunger state, and environmental risk levels. Larger $a$ strengthens this effect. As $a$ increases, the stability of the system can undergo abrupt changes, potentially leading to periodic solutions and even sustained population fluctuations. Fixing $c = 0.3$, $n = 3$, and $m = 0.5$, we obtain the threshold $a^* = 0.3079669$ and the first Lyapunov coefficient $L = -0.03425 < 0$. Hence, a stable limit cycle emerges around the positive interior equilibrium point $E_2(0.1525, 0.7754)$ for $a = 0.33 > a^*$.

(2) The parameter $c$ controls how strongly boldness amplifies the attack rate: smaller $c$ means a stronger, more rapid boldness effect that can destabilize the system, whereas larger $c$ weakens this effect and tends to promote stability. When fixing $a = 0.2$, $n = 3$, and $m = 0.5$, we obtain two thresholds $c_1^* = 1.678645$ with $L = -0.03444 < 0$ and $c_2^* = 7.047013$ with $L = -0.02823 < 0$. Thus, for $c_1^* < c = 1.72 < c_2^*$, a stable limit cycle emerges around the interior equilibrium $E_2(0.1741, 0.8629)$.

(3) The conversion efficiency $n$ governs how effectively consumed prey is converted into predator growth. Lower $n$ weakens this feedback and can promote cyclic dynamics, whereas higher $n$ strengthens predator regulation of prey and tends to stabilize coexistence. Fixing $a = 0.2$, $c = 0.3$, and $m = 0.5$, we obtain the threshold value $n^* = 4.2209$ and the first Lyapunov number $L = -0.01365 < 0$. A stable limit cycle emerges around the positive interior equilibrium point $E_2(0.1103, 0.8442)$ for $n = 4.3 > n^*$.

(4) Predator mortality $m$ also determines the stability of an ecosystem. low $m$ supports steady coexistence, moderate increases can weaken prey regulation and induce cycles, and sufficiently large $m$ drives the system to the prey-only equilibrium. Thus, external pressures that increase predator mortality, such as disease or harvesting, can shift the system from stable coexistence to oscillations or predator extinction. Here we fix $a = 0.2$, $c = 0.3$, and $n = 3$, and calculate the threshold values $m_1^* = 9.60817 * 10^{-6}$ with $L = -1.214 * 10^{-7} < 0$, and $m_2^* = 0.346073$ with $L = -0.012467 < 0$. A stable limit cycle emerges around the positive interior equilibrium point $E_2(0.0931, 0.8442)$ for $m_1^* < m = 0.3 < m_2^*$.

### 3.3.4. *Bogdanov-Takens bifurcation*

In this section, we analyze system (2.5) under small perturbations and demonstrate that it exhibits a Bogdanov-Takens (BT) bifurcation of co-dimension 2. This bifurcation captures how the system can shift between steady coexistence and sustained population oscillations. Specifically, when $n > mh$, $h = h_1$, and $m = 1 - 2u_* A_1(u_*, v_*) + nA_2(u_*, v_*)$, the system (2.5) has a cusp $E_*(u_*, v_*)$ (i.e., Bogdanov-Takens singularity). Assuming $n$ and $m$ as the as Bogdanov-Takens bifurcation parameters, we introduce the perturbed system:

$$\begin{cases} \frac{du}{dt} = u(1-u) - \frac{\left(b_0 + \frac{av}{cu+v}\right)uv}{1+\left(b_0+\frac{av}{cu+v}\right)hu}, \\ \frac{dv}{dt} = (n+\varepsilon_1)\frac{\left(b_0+\frac{av}{cu+v}\right)uv}{1+\left(b_0+\frac{av}{cu+v}\right)hu} - (m+\varepsilon_2)v, \end{cases} \tag{3.8}$$

where $(\varepsilon_1, \varepsilon_2)$ are perturbation parameters in a small neighborhood of $(0, 0)$. Additionally, let $u_1 = u - u_*$ and $v_1 = v - v_*$, the system (3.8) can be written as

$$\begin{cases} \frac{du_1}{dt} = a_1 + a_2 u_1 + a_3 v_1 + a_4 u_1^2 + a_5 u_1 v_1 + a_6 v_1^2 + P_1(u_1, v_1, \lambda_1, \lambda_2), \\ \frac{dv_1}{dt} = b_1 + b_2 u_1 + b_3 v_1 + b_4 u_1^2 + b_5 u_1 v_1 + b_6 v_1^2 + Q_1(u_1, v_1, \lambda_1, \lambda_2), \end{cases} \tag{3.9}$$

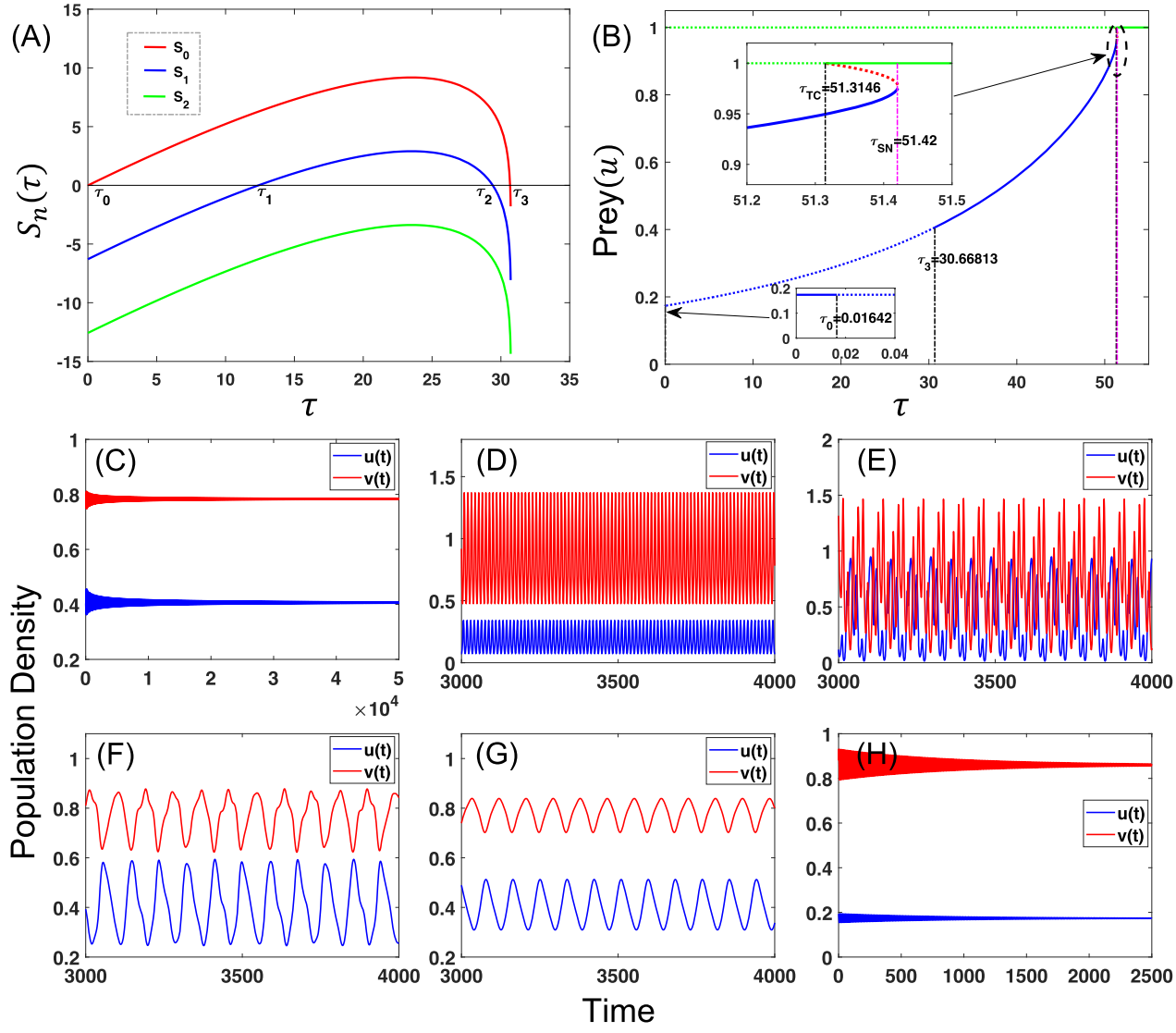


**Fig. 5.** (A) $S_n(\tau)$ plot for $n = 0, 1, 2$ under the parameter set (4.11), showing zero crossings at $\tau_0 = 0.01642$, $\tau_1 = 12.39676$, $\tau_2 = 29.40630$, and $\tau_3 = 30.66813$. (B) Bifurcation diagram in the delay $\tau$, showing a transcritical bifurcation at $\tau_{TC} = 51.3146$ and a saddle-node bifurcation at $\tau_{SN} = 51.42$. The Hopf critical values $\tau_0$ and $\tau_3$ from panel (a) align with these bifurcations. (C)-(H) Time series of prey $u(t)$ and predator $v(t)$ for representative delays: (C) $\tau = 0.01 \in (0, \tau_0)$, (D) $\tau = 0.05 \in (\tau_0, \tau_1)$, (E) $\tau = 16 \in (\tau_1, \tau_2)$, (F) $\tau = 29 \in (\tau_1, \tau_2)$, (G) $\tau = 30 \in (\tau_2, \tau_3)$, (H) $\tau = 30.7 \in (\tau_3, \hat{\tau})$.

where $P_1(u_1, v_1, \varepsilon_1, \varepsilon_2)$ and $Q_1(u_1, v_1, \varepsilon_1, \varepsilon_2)$ are $C^\infty$ functions of order at least three in $(u_1, v_1)$, and their coefficients depend smoothly on $\varepsilon_1$ and $\varepsilon_2$. The coefficients of (3.9) are given by:

$$a_1 = 0, \qquad a_2 = \left.\frac{\partial f}{\partial u}\right|_{(u_*,v_*)}, \qquad a_3 = \left.\frac{\partial f}{\partial v}\right|_{(u_*,v_*)},$$

$$a_4 = \left.\frac{\partial^2 f}{\partial u^2}\right|_{(u_*,v_*)}, \quad a_5 = \left.\frac{\partial^2 f}{\partial u \partial v}\right|_{(u_*,v_*)}, \quad a_6 = \left.\frac{\partial^2 f}{\partial v^2}\right|_{(u_*,v_*)}.$$

$$b_1 = \frac{\left(b_0 + \frac{av_*}{cu_*+v_*}\right)uv}{1 + \left(b_0 + \frac{av_*}{cu_*+v_*}\right)hu_*}\varepsilon_1 - v_*\varepsilon_2, \quad b_2 = (n+\varepsilon_1)A_1(u_*, v_*),$$

$$b_3 = (n+\varepsilon_1)A_2(u_*, v_*) - (m+\varepsilon_2), \qquad b_4 = \left(\frac{n+\varepsilon_1}{n}\right)\left.\frac{\partial^2 g}{\partial u^2}\right|_{(u_*,v_*)},$$

$$b_5 = \left(\frac{n+\varepsilon_1}{n}\right)\left.\frac{\partial^2 g}{\partial u \partial v}\right|_{(u_*,v_*)}, \qquad b_6 = \left(\frac{n+\varepsilon_1}{n}\right)\left.\frac{\partial^2 g}{\partial v^2}\right|_{(u_*,v_*)}.$$

The local bifurcation curves are derived and presented in Appendix B.

To validate the theoretical results, we conduct numerical computations. Fixing $b_0 = 1$, $h = 0.5$, $a = 6$, and $c = 2.5$, we numerically solve the nonlinear conditions $\mathrm{Tr}(J(E_*)) = 0$ and $\mathrm{Det}(J(E_*)) = 0$ and have $n_* = 3.1812866, m_* = 2.4659045, D = 1.5229 \neq 0, \mathcal{E} = 0.763 \neq 0$. According to Theorem 3.4, the system (2.5) has a codimension 2 cusp at $E_*(0.7288, 0.2549)$. Hence, $\mu_1$ and $\mu_2$ can be expressed in terms of $\varepsilon_1$ and $\varepsilon_2$ as follows:

$$\begin{cases} \mu_1 = -21.2449\varepsilon_1 + 27.4163\varepsilon_2 - 28.7057\varepsilon_1^2 + 37.0391\varepsilon_1\varepsilon_2 - 47.7917\varepsilon_2 2^2 \\ \quad +O(|\varepsilon_1, \varepsilon_2|^2), \\ \mu_2 = -7.7604\varepsilon_1 + 6.7130\varepsilon_1^2 - 7.8580\varepsilon_1\varepsilon_2 + 9.1018\varepsilon_2^2 + O(|\varepsilon_1, \varepsilon_2|^2). \end{cases}$$

Jacobian determinant is non-zero, indicating that $\mu_1$ and $\mu_2$ are functionally independent:

$$\left|\frac{\partial(\mu_1, \mu_2)}{\partial(\varepsilon_1, \varepsilon_2)}\right|_{\varepsilon=0} = \begin{vmatrix} -21.2449 & 27.4163 \\ -7.7604 & 0 \end{vmatrix} = 212.7615 \neq 0.$$

Since $d_4|_{\varepsilon=0} = 1.6152 > 0$ and $d_5|_{\varepsilon=0} = -4.6709 < 0$, it follows that $\frac{d_4}{d_5}|_{\varepsilon=0} < 0$. Hence, the system (2.5) undergoes a supercritical

**Table 1**
Summary of critical parameters $(n_*, m_*) = (3.1812886, 2.4659045)$ used in Figs. 2(C) and 4.

| Values $(\varepsilon_1, \varepsilon_2)$ | Equilibria | Characteristic | Figure |
|---|---|---|---|
| $(0,0)$ | $E_*(0.7288, 0.2549)$ | Cusp of codimension 2 | Fig. 2(C) |
| $(-0.478, -0.365)$ | — | No equilibria | Fig. 4(B) |
| $(-0.478, -0.373)$ | $E_2(0.6977, 0.2724)$ | | |
| | $E_3(0.7593, 0.2361)$ | Stable focus | Fig. 4(C) |
| $(-0.478, -0.375)$ | $E_2(0.6868, 0.2781)$ | | |
| | $E_3(0.7696, 0.2293)$ | Stable limit cycle | Fig. 4(D) |
| $(-0.478, -0.37762)$ | $E_2(0.6758, 0.2836)$ | | |
| | $E_3(0.7799, 0.2222)$ | Stable homoclinic cycle | Fig. 4(E) |
| $(-0.478, -0.38)$ | $E_2(0.6675, 0.2877)$ | | |
| | $E_3(0.7876, 0.2168)$ | Unstable focus | Fig. 4(F) |

**Table 2**
Numerical results for critical parameters $(a_*, m_*) = (6.290667, 2.349038)$.

| Values $(\varepsilon_1, \varepsilon_2)$ | Equilibria | Characteristic |
|---|---|---|
| $(-0.5, -0.038)$ | — | No equilibria |
| $(0,0)$ | $E_*(0.7225, 0.2561)$ | Cusp of codimension 2 |
| $(-0.5, -0.042)$ | $E_2(0.7141, 0.2655)$, $E_3(0.7530, 0.2418)$ | Stable focus |
| $(-0.5, -0.0428)$ | $E_2(0.7078, 0.2690)$, $E_3(0.7591, 0.2379)$ | Stable limit cycle |
| $(-0.5, -0.0441)$ | $E_2(0.7000, 0.2733)$, $E_3(0.7666, 0.2329)$ | Stable homoclinic cycle |
| $(-0.5, -0.0446)$ | $E_2(0.6975, 0.2747)$, $E_3(0.7690, 0.2313)$ | Unstable focus |

Bogdanov-Takens bifurcation near the cusp equilibrium $E_*$. The corresponding bifurcation diagram and phase portraits, as $(n, m)$ vary in a small neighborhood of the critical point $(n_*, m_*)$, are summarized in Table 1 and illustrated in Fig. 4. The bifurcation curves SN (saddle-node), H (Hopf), and HL (homoclinic loop) partition the neighborhood of $(n_*, m_*)$ in the $(n, m)$-plane into four regions (see Fig. 4(A)). Biologically, this result means that when the conversion efficiency $n$ and predator mortality $m$ are close to the BT bifurcation point $(n_*, m_*)$, even small changes in these parameters can trigger critical transitions.

When $b_0 = 1$, $h = 0.5$, $c = 2.5$, and $n = 3$ are fixed, the nonlinear system composed of $\mathrm{Tr}\left(J\left(E_*\right)\right) = 0$ and $\mathrm{Det}\left(J(E_*)\right) = 0$ can be solved numerically, resulting in critical values $a_* = 6.290667$ and $m_* = 2.349038$, with $\mathcal{D} = 1.4478 \neq 0$ and $\mathcal{E} = 0.4448 \neq 0$. Note that

$$\left|\frac{\partial(\mu_1, \mu_2)}{\partial(\varepsilon_1, \varepsilon_2)}\right|_{\varepsilon=0} = \begin{vmatrix} -4.2628 & 52.7782 \\ 3.3155 & -37.6035 \end{vmatrix} = -14.6899 \neq 0,$$

which confirms that $\mu_1$ and $\mu_2$ are functionally independent. According to Theorem 3.4, the system (2.5) has a cusp equilibrium $E_*(0.7225, 0.2561)$ of co-dimension 2. We choose $a$ and $m$ as the Bogdanov-Takens bifurcation parameters given that $d_4|_{\varepsilon=0} = -0.9462 < 0$ and $d_5|_{\varepsilon=0} = 3.6356 > 0$. Hence, the system (2.5) undergoes a supercritical Bogdanov-Takens bifurcation. The corresponding phase portraits near $E_*$, as $(a, m)$ vary in a small neighborhood of $(a_*, m_*)$, are summarized in Table 2. This shows the sensitive response of system (2.5) to changes in $a$ (the maximum increment in attack rate due to boldness) and $m$ (predator mortality).

When $b_0 = 1$, $h = 0.5$, $n = 3$, and $m = 2.5$ are fixed, the nonlinear system composed of $\mathrm{Tr}\left(J\left(E_*\right)\right) = 0$ and $\mathrm{Det}\left(J(E_*)\right) = 0$ can be solved numerically, yielding the critical values $a_* = 4.1751886, c_* = 1.0897812, \mathcal{D} = 1.1488 \neq 0, \mathcal{E} = -0.4521 \neq 0$. Similarly, the Jacobian determinant

$$\left|\frac{\partial(\mu_1, \mu_2)}{\partial(\varepsilon_1, \varepsilon_2)}\right|_{\varepsilon=0} = \begin{vmatrix} -0.7781 & 2.2935 \\ 1.2598 & -0.5696 \end{vmatrix} = -2.4461 \neq 0,$$

confirms that $\mu_1$ and $\mu_2$ are functionally independent. According to Theorem 3.4, the system (2.5) has a cusp $E_*(0.7258, 0.2388)$ of codimension 2. We choose $a$ and $c$ as Bogdanov-Takens bifurcation parameters given that $d_4|_{\varepsilon=0} = -1.1815 < 0$, $d_5|_{\varepsilon=0} = 2.4857 > 0$ $(\frac{d_4}{d_5}|_{\varepsilon=0} < 0)$. Hence, the system (2.5) undergoes a supercritical Bogdanov-Takens bifurcation. The corresponding phase portraits near $E_*$, as $(a, c)$ vary in a small neighborhood of $(a_*, c_*)$, are presented in Table 3. This highlights the sensitivity of system (2.5) to variations in $a$ (the maximal increase in attack rate induced by boldness) and $c$ (the half-saturation constant governing how strongly boldness amplifies the attack rate).

**Table 3**
Numerical results for critical parameters $(a_*, c_*) = (4.1751886, 1.0897812)$.

| Values $(\varepsilon_1, \varepsilon_2)$ | Equilibria | Characteristic |
|---|---|---|
| $(-0.5, -0.165)$ | — | No equilibria |
| $(0,0)$ | $E_*(0.7258, 0.2388)$ | Cusp of codimension 2 |
| $(-0.5, -0.173)$ | $E_2(0.7130, 0.2456)$, $E_3(0.7560, 0.2214)$ | Stable focus |
| $(-0.5, -0.1735)$ | $E_2(0.7115, 0.2463)$, $E_3(0.7573, 0.2205)$ | Stable limit cycle |
| $(-0.5, -0.1773)$ | $E_2(0.7026, 0.2508)$, $E_3(0.7656, 0.2153)$ | Stable homoclinic cycle |
| $(-0.5, -0.1788)$ | $E_2(0.6996, 0.2522)$, $E_3(0.7683, 0.2136)$ | Unstable focus |

## 4. Dynamics with maturation delay

### 4.1. Preliminaries

To investigate the positivity and boundedness of solutions, as well as the equilibria of system (2.6) under nonnegative initial conditions, we define the Banach space $\mathcal{C} := C([-\tau, 0], \mathbb{R})$ as the space of continuous functions on $[-\tau, 0]$ for any $\tau > 0$, with the norm defined by

$$|\varphi| = \sup_{\theta \in [-\tau, 0]} |\varphi(\theta)| \ \textit{for any } \varphi \in \mathcal{C}.$$

Let $\mathcal{C}^+ := C([-\tau, 0], \mathbb{R}_+)$ denote the nonnegative cone of $\mathcal{C}$, where $\mathbb{R}_+ = [0, \infty)$, and define $\varphi_t(\theta) := \varphi(t + \theta)$ for $\theta \in [-\tau, 0]$. Biologically, the admissible initial conditions for system (2.6) are given by

$$(u_0, v_0) \in X := \mathcal{C}^+ \times \mathcal{C}^+.$$

Applying the standard theory of functional differential equations, we get following result:

**Theorem 4.1.** *The solution of system (2.6) with initial conditions $(u(\theta), v(\theta)) \in X$ are nonnegative, and the region*

$$\Gamma = \left\{ (u, v) \in X : \|u\| \leq 1, \|v\| \leq \frac{ne^{-\delta\tau}}{\min\{1, m\}} \right\},$$

*is positively invariant and absorbing in $X$; that is, all solutions eventually enter and remain in $\Gamma$.*

**Proof.** Since $u(t), v(t)$ are continuous and $u(0), v(0) > 0$, the positivity of $u(t)$ can be derived from the following fact

$$u(t) = u(0) exp\left( \int_0^t \left( u(s)(1 - u(s)) - \frac{\beta(u(s), v(s))u(s)v(s)}{1 + \beta(u(s), v(s))hu(s)} \right) ds \right),$$

$$for\ all\ t > 0.$$

For $t \in [0, \tau]$, $v(t)$ satisfies $\dot{v}(t) \geq -mv(t)$, which yields $v(t) \geq v(0)e^{-mt} > 0$ for all $t \in [0, \infty)$. Therefore, $u(t) > 0$ and $v(t) > 0$ for all $t \geq 0$, which implies $\lim_{t \to +\infty} \sup u(t) \leq 1$.

Define $W(t) = ne^{-\delta\tau}u(t) + v(t + \tau)$, then we have

$$\begin{aligned} \frac{dW(t)}{dt} &= ne^{-\delta\tau}u(t)(1 - u(t)) - mv(t + \tau) \\ &\leq ne^{-\delta\tau}(1 - u(t)) - mv(t + \tau) \leq ne^{-\delta\tau} - \min\{1, m\}\left(ne^{-\delta\tau}u(t) + v(t + \tau)\right), \end{aligned}$$

and thus

$$\lim_{t \to +\infty} \sup W(t) \leq \frac{ne^{-\delta\tau}}{\min\{1, m\}},$$

which further implies

$$\lim_{t \to +\infty} \sup v(t) \leq \frac{ne^{-\delta\tau}}{\min\{1, m\}}.$$

Thus $x(t), y(t)$ are ultimately bounded. □

### 4.2. Equilibria and their stability

The system (2.6) always has a trivial equilibrium $E_{\tau 0}(0,0)$ and a boundary equilibrium $E_{\tau 1}(1,0)$. In align with the discussion of the number of positive equilibrium points in Section 3.2, we still assume that $E_\tau(u,v)$ is a positive equilibrium of system (2.6). Then $u$ must be a real root of the following quadratic equation:

$$F_\tau(u) = \alpha_\tau u^2 - \beta_\tau u + \gamma_\tau = 0, (0 < u < 1), \tag{4.1}$$

where

$$\alpha_\tau = \left(ne^{-\delta\tau} - mh\right)(b_0 + a)n,$$
$$\beta_\tau = mn + \left(ne^{-\delta\tau} - mh\right)\left[b_0 mce^{\delta\tau} + n\left(b_0 + a\right)\right],$$
$$\gamma_\tau = m\left(mce^{\delta\tau} + n\right).$$

While our focus is on the delay parameter $\tau$, it is important to note that parameters in the functional response, such as $h$, also affect the number and stability of equilibria in system (2.6).

To ensure that $v = \frac{(ne^{-\delta\tau} - mh)b_0 cu^2 - mcu}{m - (ne^{-\delta\tau} - mh)(b_0 + a)} > 0$, one prerequisite is $h < \frac{n}{m}e^{-\delta\tau}$. Hence, according to the roots formula of the second-order linear algebraic equation, we get

$$\Delta_\tau = \beta_\tau^2 - 4\alpha_\tau\gamma_\tau = \left\{mn + \left(ne^{-\delta\tau} - mh\right)\left[b_0 mce^{\delta\tau} + n(b_0 + a)\right]\right\}^2 - 4mn\left(ne^{-\delta\tau} - mh\right)\left(b_0 + a\right)\left(mce^{\delta\tau} + n\right).$$

In analogy with Lemmas 3.1 and 3.2, we also treat $h$ as a bifurcation parameter and define the function:

$$\mathbf{F}_\tau(h) = P_{\tau,h}h^2 - Q_{\tau,h}h + R_{\tau,h} = 0, \tag{4.2}$$

where

$$P_{\tau,h} = m^2\left[b_0 mce^{\delta\tau} + n(b_0 + a)\right]^2 > 0,$$
$$Q_{\tau,h} = 2mne^{-\delta\tau}\left[b_0 mce^{\delta\tau} + n(b_0 + a)\right]^2 + 2m^2 n\left[b_0 mce^{\delta\tau} + n(b_0 + a)\right] - 4m^2 n(b_0 + a)\left(mce^{\delta\tau} + n\right),$$
$$R_{\tau,h} = m^2 n^2 + 2mn^2 e^{-\delta\tau}\left[b_0 mce^{\delta\tau} + n(b_0 + a)\right] + n^2 e^{-2\delta\tau}\left[b_0 mce^{\delta\tau} + n(b_0 + a)\right]^2 - 4mn^2 e^{-\delta\tau}(b_0 + a)(mce^{\delta\tau} + n).$$

Use the discriminant $\Delta_\tau$ of (4.1) and let

$$h_{\tau,1} = \frac{Q_{\tau,h} - \sqrt{\Delta_{\tau,h}}}{2P_{\tau,h}}, \quad h_{\tau,2} = \frac{Q_{\tau,h} + \sqrt{\Delta_{\tau,h}}}{2P_{\tau,h}}, \quad \Delta_{\tau,h} = Q_{\tau,h}^2 - 4P_{\tau,h}R_{\tau,h},$$

we obtain the following results:

**Lemma 4.1.** *When $h < \frac{n}{m}e^{-\delta\tau}$, this is $0 < \tau < \frac{1}{\delta}ln\frac{n}{mh}$, the positive roots of the system (4.2) as follows:*

*(i) If $\Delta_{\tau,h} > 0, R_{\tau,h} > 0$ and $0 < \frac{Q_{\tau,h}}{2P_{\tau,h}} < \frac{n}{m}e^{-\delta\tau}$, then the system (4.2) has two positive equilibria $h_{\tau,1}$ and $h_{\tau,2}$ with $h_{\tau,1} < h_{\tau,2}$;*

*(ii) If $\Delta_{\tau,h} = 0, R_{\tau,h} > 0$ and $0 < \frac{Q_{\tau,h}}{2P_{\tau,h}} < \frac{n}{m}e^{-\delta\tau}$, then the system (4.2) has one positive equilibrium $h_{\tau,1} = h_{\tau,2} = \frac{Q_{0,h}}{2P_{0,h}}$;*

*(iii) If $\mathbf{F}_\tau(0) < 0$, then the system (4.2) has one positive equilibrium $h_{\tau,2}$.*

From a biological standpoint, we are interested only in the interval $u \in (0,1)$ and $h_{\tau,2}$ actually does not exist. We present a concise justification below. Define the function

$$h(u) = \frac{ne^{-\delta\tau}}{m} - \frac{1}{uG(u)}, \quad G(u) = b_0 + \frac{ane^{-\delta\tau}(1-u)}{mc + ne^{-\delta\tau}(1-u)} > 0, \quad u \in (0,1).$$

Solving $G(u) = 0$, we obtain

$$u_{\tau**} = 1 + \frac{b_0 mc}{ne^{-\delta\tau}(b_0 + a)} > 1.$$

Then differentiating $h(u)$ with respect to $u$ yields:

$$h'(u) = \frac{G(u) + uG'(u)}{(uG(u))^2}, \quad G'(u) = -\frac{amne^{-\delta\tau}c}{\left(mc + ne^{-\delta\tau}(1-u)\right)^2} < 0.$$

Moreover, consider the limit process of $h(u)$ with respect to $u$:

$$\lim_{u\to 0^+} h(u) = -\infty, \quad \lim_{u\to 1^-} h(u) = \frac{ne^{-\delta\tau}}{m} - \frac{1}{b_0}, \quad \lim_{u\to u_{\tau**}^-} h(u) = -\infty,$$

and

$$\lim_{u\to+\infty} h(u) = \frac{ne^{-\delta\tau}}{m}, \quad \lim_{u\to u_{\tau**}^+} h(u) = +\infty.$$

This implies that there exists $u_{\tau 0} \in (0,1)$ such that $h'(u_{\tau 0}) = 0$. Consequently, only the root $h_{\tau,1}$ lies within the biologically feasible domain, and $h_{\tau,2}$ must be discarded. The number of positive equilibria of system (2.6) is characterized as follows:

**Lemma 4.2.** *For the system (2.6), we have*

*(i) If $\frac{n}{m}e^{-\delta\tau} - \frac{1}{b_0} < h < \frac{n}{m}e^{-\delta\tau}$, that is, $\frac{1}{\delta}ln\frac{nb_0}{m(hb_0+1)} < \tau < \frac{1}{\delta}ln\frac{n}{mh}$, then:*

*(i1) System (2.6) has no positive equilibria for $h > h_{\tau 1}$;*

*(i2) System (2.6) has an unique positive equilibrium*

$$E_{\tau*}(u_{\tau*}, v_{\tau*}) = E_{\tau*}\left(\frac{\beta_\tau}{2\alpha_\tau}, \frac{ne^{-\delta\tau}\beta_\tau(2\alpha_\tau - \beta_\tau)}{4m\alpha_\tau^2}\right)$$

*for $h = h_{\tau 1}$;*

*(i3) System (2.6) has two positive equilibria $E_{\tau 2}(u_{\tau 2}, v_{\tau 2})$ and $E_{\tau 3}(u_{\tau 3}, v_{\tau 3})$ for $h < h_{\tau 1}$, where*

$$u_{\tau 2} = \frac{\beta_\tau - \sqrt{\beta_\tau^2 - 4\alpha_\tau\gamma_\tau}}{2\alpha_\tau}, \quad v_{\tau 2} = \frac{ne^{-\delta\tau}u_{\tau 2}(1-u_{\tau 2})}{m};$$
$$u_{\tau 3} = \frac{\beta_\tau + \sqrt{\beta_\tau^2 - 4\alpha_\tau\gamma_\tau}}{2\alpha_\tau}, \quad v_{\tau 3} = \frac{ne^{-\delta\tau}u_{\tau 3}(1-u_{\tau 3})}{m}.$$

*(ii) If $0 < h < \frac{n}{m}e^{-\delta\tau} - \frac{1}{b_0}$, that is, $0 < \tau < \frac{1}{\delta}ln\frac{nb_0}{m(hb_0+1)}$, then the system (2.6) has one positive equilibria $E_{\tau 2}(u_{\tau 2}, v_{\tau 2})$.*

**Proof.** A necessary condition for the existence of positive equilibria is $h < \frac{ne^{-\delta\tau}}{m}$, ensuring that

$$v = \frac{\left(ne^{-\delta\tau} - mh\right)b_0 cu^2 - mcu}{m - \left(ne^{-\delta\tau} - mh\right)(b_0 + a)} > 0.$$

Since $\alpha_\tau$, $\beta_\tau$, and $\gamma_\tau > 0$, we have

$$F_\tau(0) > 0, \quad \frac{\beta_\tau}{2\alpha_\tau} > 0, \quad F_\tau(1) = mc\left(m - \left(ne^{-\delta\tau} - mh\right)b_0\right).$$

If $F_\tau(1) > 0$, i.e. $h > \frac{ne^{-\delta\tau}}{m} - \frac{1}{b_0}$, then system (4.1) has either (a) no positive root when $\Delta_\tau < 0$ ($h > h_{\tau 1}$); (b) a unique positive root when $\Delta_\tau = 0$ ($h = h_{\tau 1}$); or (c) two positive roots when $\Delta_\tau > 0$ ($h < h_{\tau 1}$). On the other hand, if $F_\tau(1) < 0$, i.e., $h < \frac{ne^{-\delta\tau}}{m} - \frac{1}{b_0}$, then $F_\tau(u)$ must intersect the $u$-axis, and thus system (4.1) admits a unique positive root. □

Lemma 4.2 converts the $h$ condition for positive equilibria into an equivalent range of delays $\tau \in [0, \tau_{\max}]$. Within this interval, system (2.6) admits

$$\begin{cases} \text{one positive equilibrium } E_{\tau 2}, & 0 \le \tau < \tau_{TC}, \\ \text{two positive equilibria } E_{\tau 2}, E_{\tau 3}, & \tau_{TC} < \tau < \tau_{SN}, \\ \text{none}, & \tau_{SN} < \tau \le \tau_{\max}. \end{cases}$$

Hence a transcritical bifurcation occurs at

$$\tau_{TC} = \frac{1}{\delta}\ln\left(\frac{nb_0}{m(hb_0+1)}\right),$$

where the positive branch meets the boundary equilibrium, while a saddle-node bifurcation occurs at

$$\tau_{SN} := \{\tau \mid \Delta_{\tau,h} = 0\},$$

where the two interior equilibria merge. The admissible delay is bounded above by

$$\tau_{\max} = \frac{1}{\delta}\ln\left(\frac{n}{mh}\right).$$

Next, we study the local stability of each equilibrium. The linearization of system (2.6) in the vicinity of the any equilibrium $E_\tau(u,v)$ yields:

$$\begin{cases} \frac{du(t)}{dt} = a_1 u(t) + a_2 v(t), \\ \frac{dv(t)}{dt} = b_1 u(t-\tau) + b_2 v(t-\tau) + b_3 v(t), \end{cases} \tag{4.3}$$

where

$$a_1 = 1 - 2u - A_1(u,v), \quad a_2 = -A_2(u,v),$$
$$b_1 = ne^{-\delta\tau} A_1(u,v), \quad b_2 = ne^{-\delta\tau} A_2(u,v), \quad b_3 = -m,$$

with

$$A_1(u,v) = \frac{\left[\left(b_0 + \frac{av}{cu+v}\right) - \frac{acuv}{(cu+v)^2}\right]v}{\left[1 + \left(b_0 + \frac{av}{cu+v}\right)hu\right]^2},$$

$$A_2(u,v) = \frac{\frac{acu^2v}{(cu+v)^2} + \left(b_0 + \frac{av}{cu+v}\right)u + \left(b_0 + \frac{av}{cu+v}\right)^2 hu^2}{\left[1 + \left(b_0 + \frac{av}{cu+v}\right)hu\right]^2}.$$

The characteristic equation associated with system (4.3) is given by

$$\mathbf{\Delta}(\lambda,\tau) = \mathbf{\Delta}_1(\lambda,\tau) + e^{-\lambda\tau}\mathbf{\Delta}_2(\lambda,\tau) = 0, \tag{4.4}$$

with

$$\begin{cases} \mathbf{\Delta}_1(\lambda,\tau) = \lambda^2 + \mathbf{a}(\tau)\lambda + \mathbf{b}(\tau), \\ \mathbf{a}(\tau) = -\left(a_1 + b_3\right), \quad \mathbf{b}(\tau) = a_1 b_3, \end{cases} \quad \begin{cases} \mathbf{\Delta}_2(\lambda,\tau) = \mathbf{c}(\tau)\lambda + \mathbf{d}(\tau), \\ \mathbf{c}(\tau) = -b_2, \quad \mathbf{d}(\tau) = a_1 b_2 - a_2 b_1. \end{cases}$$

At the trivial equilibrium point $E_{\tau 0}(0,0)$, we have $a_1 = 1, a_2 = 0, b_1 = 0, b_2 = 0, b_3 = -m$, which is evident that $E_{\tau 0}(0,0)$ is always an unstable. The internalized system (2.6) around $E_{\tau 1}(1,0)$ becomes

$$\begin{cases} \frac{du(t)}{dt} = -u(t) - \frac{b_0}{1+b_0 h} v(t), \\ \frac{dv(t)}{dt} = \frac{nb_0}{1+b_0 h} e^{-\delta\tau} v(t-\tau) - mv(t), \end{cases} \tag{4.5}$$

with two eigenvalue $\lambda = -\left(m - \frac{nb_0}{1+b_0 h} e^{-\delta\tau}\right)$ and $\lambda = -1$ of the characteristic equation of system (4.5). Hence, $E_{\tau 1}(1,0)$ is stable for $m > \frac{nb_0}{1+b_0 h} e^{-\delta\tau}$ $\left(i.e., \tau > \frac{1}{\delta} ln \frac{nb_0}{m(hb_0+1)}\right)$ and is unstable otherwise. The predator-free equilibrium loses stability via a transcritical bifurcation at $\tau = \frac{1}{\delta} ln \frac{nb_0}{m(hb_0+1)}$ where $m - \frac{nb_0}{1+b_0 h} e^{-\delta\tau} = 0$.

To summarize, we state the local stability of $E_{\tau 0}$ and $E_{\tau 1}$ of system (2.6) as follows:

**Theorem 4.2.** *System (2.6) always has two boundary equilibria: $E_{\tau 0}(0,0)$ and $E_{\tau 1}(1,0)$. Moreover, $E_{\tau 0}(0,0)$ is always an unstable node for $\tau > 0$, and*

*(i) $E_{\tau 1}(1,0)$ is a saddle for $\tau \in \left(0, \frac{1}{\delta} ln \frac{nb_0}{m(hb_0+1)}\right)$;*

*(ii) $E_{\tau 1}(1,0)$ is a stable node for $\tau \in \left(\frac{1}{\delta} ln \frac{nb_0}{m(hb_0+1)}, +\infty\right)$;*

*(iii) $E_{\tau 1}(1,0)$ undergoes a transcritical bifurcation at $\tau_{TC} = \frac{1}{\delta} ln \frac{nb_0}{m(hb_0+1)}$.*

Theorem 4.2 shows that the extinction equilibrium $E_{\tau 0}(0,0)$ does not depend on the time delay. Its instability persists for all $\tau > 0$. In contrast, the prey-only equilibrium $E_{\tau 1}(1,0)$ is delay-dependent because the predator recruitment term is discounted by the survival factor $e^{-\delta\tau}$. As $\tau$ increases, $E_{\tau 1}$ switches from a saddle to a stable node. The critical delay $\tau_{TC}$ therefore marks a transcritical bifurcation at which the system transitions between predator persistence and predator extinction.

By Theorem 3.3, $E_3$ is unstable at $\tau = 0$, so its delayed counterpart $E_{\tau 3}$ remains unstable for all $\tau \in (\tau_{TC}, \tau_{SN})$. In contrast, the stability of the positive equilibrium $E_{\tau 2}$ can vary and gives rise to richer dynamics. In the following, we further investigate $E_{\tau 2}$ and assume $\tau \in (0, \tau_{max})$, where positive equilibria exist.

### 4.3. Hopf bifurcation analysis

#### 4.3.1. Stability and Hopf bifurcation

Following the approach in [31], we investigate the conditions under which a Hopf bifurcation occurs in system (2.6) due to the time delay $\tau$. We substitute $\lambda = i\omega$ into (4.4) and obtain

$$\Delta(i\omega,\tau) = \mathcal{P}(i\omega,\tau) + e^{-i\omega\tau}\mathcal{Q}(i\omega,\tau) = 0,$$

where $\omega \in R^+$ and $\Delta(i\omega,\tau) = 0$. Separating real $(R)$ and imaginary $(I)$ parts leads to

$$\begin{cases} \mathcal{P}_R(i\omega,\tau) + \mathcal{Q}_R(i\omega,\tau)\cos\omega\tau + \mathcal{Q}_I(i\omega,\tau)\sin\omega\tau = 0, \\ \mathcal{P}_I(i\omega,\tau) + \mathcal{Q}_I(i\omega,\tau)\cos\omega\tau - \mathcal{Q}_R(i\omega,\tau)\sin\omega\tau = 0, \end{cases}$$

where

$$\mathcal{P}_R(i\omega,\tau) = b(\tau) - \omega^2, \quad \mathcal{P}_I(i\omega,\tau) = a(\tau)\omega,$$
$$\mathcal{Q}_R(i\omega,\tau) = d(\tau), \quad \mathcal{Q}_I(i\omega,\tau) = c(\tau)\omega.$$

As a result, we get

$$\begin{cases} \sin(\omega\tau) = \frac{\mathcal{P}_I(i\omega,\tau)\mathcal{Q}_R(i\omega,\tau) - \mathcal{P}_R(i\omega,\tau)\mathcal{Q}_I(i\omega,\tau)}{\mathcal{Q}_R^2(i\omega,\tau) + \mathcal{Q}_I^2(i\omega,\tau)} = \mathcal{F}_s(\omega,\tau), \\ \cos(\omega\tau) = -\frac{\mathcal{P}_R(i\omega,\tau)\mathcal{Q}_R(i\omega,\tau) + \mathcal{P}_I(i\omega,\tau)\mathcal{Q}_I(i\omega,\tau)}{\mathcal{Q}_R^2(i\omega,\tau) + \mathcal{Q}_I^2(i\omega,\tau)} = \mathcal{F}_c(\omega,\tau), \end{cases} \tag{4.6}$$

By squaring and summing both equations in (4.6), we obtain the following polynomial for $\omega$:

$$\mathcal{F}(\omega,\tau) = \omega^4 + \mathcal{A}(\omega,\tau)\omega^2 + \mathcal{B}(\omega,\tau) = 0, \tag{4.7}$$

where

$$\mathcal{A}(\omega,\tau) = a(\tau)^2 - c(\tau)^2 - 2b(\tau), \quad \mathcal{B}(\omega,\tau) = b(\tau)^2 - d(\tau)^2.$$

Next, to analyze the existence of positive zeros of Eq. (4.7), we introduce the following assumptions:

$(\mathcal{H}_1)$ $a(0) + c(0) > 0$ and $b(0) + d(0) > 0$;
$(\mathcal{H}_2)$ Either $\mathcal{A}(\omega,\tau) > 0$ and $\mathcal{B}(\omega,\tau) > 0$ or $\mathcal{A}(\omega,\tau)^2 - 4\mathcal{B}(\omega,\tau) < 0$;
$(\mathcal{H}_3)$ Either $\mathcal{B}(\omega,\tau) < 0$ or $\mathcal{A}(\omega,\tau) < 0$ and $\mathcal{A}(\omega,\tau)^2 - 4\mathcal{B}(\omega,\tau) = 0$;
$(\mathcal{H}_4)$ $\mathcal{B}(\omega,\tau) > 0$, $\mathcal{A}(\omega,\tau) < 0$ and $\mathcal{A}(\omega,\tau)^2 - 4\mathcal{B}(\omega,\tau) > 0$.

We now count the number of simple positive roots for $\mathcal{F}(\omega,\tau)$ in following lemma.

**Lemma 4.3.** *For Eq. (4.7), we have:*

*(i) If $(\mathcal{H}_1)$ and $(\mathcal{H}_2)$ hold, then $\mathcal{F}(\omega,\tau)$ has no positive root;*
*(ii) If $(\mathcal{H}_1)$ and $(\mathcal{H}_3)$ hold, then $\mathcal{F}(\omega,\tau)$ has exactly one simple positive root $\omega_+$;*
*(iii) If $(\mathcal{H}_1)$ and $(\mathcal{H}_4)$ hold, then $\mathcal{F}(\omega,\tau)$ has two distinct simple positive roots $\omega_\pm$,*

*where*

$$\omega_\pm(\tau) = \sqrt{\frac{-\mathcal{A}(\omega,\tau) \pm \sqrt{\mathcal{A}(\omega,\tau)^2 - 4\mathcal{B}(\omega,\tau)}}{2}}.$$

We now focus on the Hopf bifurcation analysis when $(\mathcal{H}_1)$ and $(\mathcal{H}_3)$ hold. Let

$$I_1 = \{\tau : F(\omega,\tau) = 0 \ has \ exactly \ one \ simple \ positive \ \text{root} \ \omega_+ \ for \ \tau \in [0, \tau_{SN})\}.$$

For each $\tau \in I_1$, let $\theta(\tau)$ be the unique solution of $\sin(\theta(\tau)) = \mathcal{F}_s(\omega,\tau)$ and $\cos(\theta(\tau)) = \mathcal{F}_c(\omega,\tau)$ in $(0, 2\pi]$, given by

$$\theta(\tau) = \begin{cases} \arccos \mathcal{F}_c, & \mathcal{F}_s > 0, \\ 2\pi - \arccos \mathcal{F}_c, & \mathcal{F}_s < 0. \end{cases} \tag{4.8}$$

From Beretta and Kuang [31], we define

$$\mathcal{S}_n(\tau) = \omega(\tau)\tau - \theta(\tau) - 2n\pi, \ for \ \tau \in I_1 \ with \ n \in \mathcal{N}_0. \tag{4.9}$$

One can verify that $\pm i\omega(\tau^*)$ are a pair of purely imaginary eigenvalues of (4.4) if and only if $\mathcal{S}_n(\tau^*) = 0$ for some $n \in \mathcal{N}_0$. According to Beretta and Kuang [31], the transversality condition is given by

$$Sign\left\{\frac{d\,Re\lambda}{d\tau}|_{\lambda=i\omega(\tau^*)}\right\} = Sign\left\{\frac{\partial \mathcal{F}}{\partial \omega}\left(\omega(\tau^*),\tau^*\right)\right\} Sign\left\{\mathcal{S}_n'(\tau^*)\right\}.$$

Assumption $(\mathcal{A}_1)$ Denote $\hat{\tau} = \sup I_1$, $\tau \in I_1 = [0,\hat{\tau})$, $\sup_{\tau\in I_1}\mathcal{S}_0(\tau) > 0$, and $\mathcal{S}_n(\tau)$ has at most two zeros (counting multiplicity) for any $n \in N$.

$(\mathcal{A}_1)$ implies that there exists a positive integer $K_1$, $\mathcal{S}_n(\tau)$ has two simple zeros $\tau_n$ and $\tau_{2K_1-1-n}\left(0 \le n \le K_1-1\right)$. Since $\mathcal{S}_n(\tau)$ is strictly decreasing in $n$, then we have $0 < \tau_0 < \tau_1 < \cdots < \tau_{2K_1-1} < \hat{\tau}$. Moreover, $\mathcal{S}_n'(\tau_n) > 0$ and $\mathcal{S}_n'\left(\tau_{2K_1-1-n}\right) < 0$. It then follows that a pair of purely imaginary eigenvalues $\pm i\omega(\tau)$ of (4.4) cross the imaginary axis from left to right at $\tau_n$ when $n = 0, 1, \ldots, K_1-1$, and a pair of purely imaginary eigenvalues $\pm i\omega(\tau)$ of (4.4) cross the imaginary axis from right to left at $\tau_n$ when $n = K_1, \ldots, 2K_1-1$. Hence, system (2.6) undergoes a Hopf bifurcation at $E_2$ when $\tau_n$ with $1 \le n \le 2K_1-1$.

**Theorem 4.3.** *Assume that system (2.6) satisfies hypothesis $(\mathcal{H}_1)$ and $(\mathcal{H}_3)$, and let $\mathcal{S}_n(\tau)$ be defined by (4.9).*

*(i) If $\sup_{\tau\in I_1}\mathcal{S}_0(\tau) \le 0$, then $E_{\tau 2}$ is locally asymptotically stable for all $\tau \in [0,\tau_{SN})$.*

*(ii) If $\sup_{\tau\in I_1}\mathcal{S}_0(\tau) > 0$, and $\mathcal{S}_n(\tau)$ has at most two zeros in $I_1$ (counting multiplicity) for each $n \in \mathcal{N}_0$, then there exist exactly $2K_1$ Hopf bifurcation values $\tau_0 < \tau_1 < \cdots < \tau_{2K_1-1}$, at which Hopf bifurcation occur. Moreover, $E_{\tau 2}$ is locally asymptotically stable for $\tau \in [0,\tau_0) \cup \left(\tau_{2K_1-1},\tau_{SN}\right)$, and unstable for $\tau \in \left(\tau_0,\tau_{2K_1-1}\right)$.*

Theorem 4.3 implies that this delayed response is not always destabilizing, but it can be strong enough for certain delay lengths to generate persistent oscillations. The model reveals intervals of $\tau$ where coexistence is stable, and other intervals where delayed feedback drives recurrent cycles.

### 4.3.2. Stability switches

We now analyze the stability switches of $E_{\tau 2}$ by examining the characteristic Eq. (4.4). Let

$$I_2 = \{\tau : \mathcal{F}(\omega,\tau) = 0 \text{ has two simple positive roots } \omega_\pm \text{ for } \tau \in [0,\tau_{SN})\}.$$

We denote

$$\widetilde{\tau} = \sup I_2,$$

For $\tau \in I_2$, $\mathcal{F}(\omega,\tau) = 0$ has two simple positive roots, denoted by $\omega_-(\tau) < \omega_+(\tau)$. Then $\theta_\pm$ are defined via (4.8) for $\omega = \omega_\pm$. Similar to (4.9), we define

$$\mathcal{S}_n^\pm(\tau) = \omega_\pm(\tau)\tau - \theta_\pm(\tau) - 2n\pi, \quad \tau \in [0,\widetilde{\tau}),\ n \in \mathbb{N}_0. \tag{4.10}$$

Since $\omega_-(\tau) < \omega_+(\tau)$, we have $\mathcal{F}'(\omega_-(\tau),\tau) < 0$ and $\mathcal{F}'(\omega_+(\tau),\tau) > 0$. If $\mathcal{S}_n^\pm(\tau)$ has a positive zero $\tau^\pm$, then the characteristic Eq. (4.9) has a pair of simple purely imaginary eigenvalues $\pm i\omega_\pm(\tau^\pm)$ at $\tau = \tau^\pm$, with

$$Sign\left\{\frac{d\,Re\lambda}{d\tau}|_{\lambda=i\omega_+(\tau^+)}\right\} = Sign\left\{\frac{d\,\mathcal{S}_n^+(\tau^+)}{d\tau}\right\},$$

$$Sign\left\{\frac{d\,Re\lambda}{d\tau}|_{\lambda=i\omega_-(\tau^-)}\right\} = -Sign\left\{\frac{d\,\mathcal{S}_n^-(\tau^-)}{d\tau}\right\}.$$

Assumption $(\mathcal{A}_2)$ $\mathcal{S}_0^+(\tau) > \mathcal{S}_0^-(\tau)$, $\tau \in I_2 = [0,\widetilde{\tau})$, $\sup_{\tau\in I_2}\mathcal{S}_0^+(\tau) > 0$, and $\mathcal{S}_n^\pm(\tau)$ has at most two zeros (counting multiplicity) for any $n \in N$.

Define

$$K_2 := \max\left\{n \in N_0 : \sup_{\tau\in I_2}\mathcal{S}_n^+(\tau) > 0\right\}.$$

Under $(\mathcal{A}_2)$, since $\mathcal{S}_0^\pm(0) < 0$, $\mathcal{S}_n^+(\tau) > \mathcal{S}_n^-(\tau)$, and $\mathcal{S}_n^\pm(\tau) = \mathcal{S}_0^\pm(\tau) - 2n\pi$ for $\tau \in I_2$, the functions $\mathcal{S}_n^\pm(\tau)$ (for $0 \le n \le K_2-1$) each have exactly two zeros, denoted by $\tau_n^\pm$, with $\mathrm{Re}\,\lambda'(\tau_n^+) > 0$ and $\mathrm{Re}\,\lambda'(\tau_n^-) < 0$.

If $\lim_{\tau\to\widetilde{\tau}}\mathcal{S}_{K_2}^-(\tau) > 0$, then $\mathcal{S}_{K_2}^\pm(\tau)$ has exactly two zeros $\tau_{K_2}^\pm$ with $\mathrm{Re}\,\lambda'(\tau_{K_2}^+) > 0$ and $\mathrm{Re}\,\lambda'(\tau_{K_2}^-) < 0$. Otherwise, if $\lim_{\tau\to\widetilde{\tau}}\mathcal{S}_{K_2}^-(\tau) < 0$, then $\mathcal{S}_{K_2}^+(\tau)$ has two zeros $\tau_{K_2,1}^+$ and $\tau_{K_2,2}^+$ with $\mathrm{Re}\,\lambda'(\tau_{K_2,1}^+) > 0$ and $\mathrm{Re}\,\lambda'(\tau_{K_2,2}^+) < 0$.

Hence, we derive the following Hopf bifurcation and multiple stability switches theorem.

**Theorem 4.4.** *Consider system (2.6) under assumptions $(\mathcal{H}_1)$ and $(\mathcal{H}_4)$, and let $\mathcal{S}_n^\pm(\tau)$ be defined in (4.10).*

*(i) Suppose that $\mathcal{S}_0^-(\tau) > \mathcal{S}_1^+(\tau)$ for $\tau \in I_2$. Then:*

*(i1) If $\lim_{\tau\to\widetilde{\tau}}\mathcal{S}_{K_2}^-(\tau) < 0$, then there exist $2K_2+2$ distinct Hopf bifurcation values and stability switches of $E_{\tau 2}$:*

$$\tau_0^+ < \tau_0^- < \cdots < \tau_{K_2,1}^+ < \tau_{K_2,2}^+.$$

*In this case, $E_{\tau 2}$ is locally asymptotically stable for*

$$\tau \in [0,\tau_0^+) \cup (\tau_0^-,\tau_1^+) \cup \cdots \cup (\tau_{K_2-1}^-,\tau_{K_2,1}^+) \cup (\tau_{K_2,2}^+,\tau_{\mathrm{SN}}),$$

*and unstable for*

$$\tau \in (\tau_0^+,\tau_0^-) \cup \cdots \cup (\tau_{K_2,1}^+,\tau_{K_2,2}^+).$$

*(i2) If $\lim_{\tau\to\widetilde{\tau}}\mathcal{S}_{K_2}^-(\tau) > 0$, then the Hopf bifurcation values and stability switches of $E_{\tau 2}$ are:*

$$\tau_0^+ < \tau_0^- < \cdots < \tau_{K_2}^+ < \tau_{K_2}^-.$$

*In this case, $E_{\tau 2}$ is locally asymptotically stable for*

$$\tau \in [0,\tau_0^+) \cup (\tau_0^-,\tau_1^+) \cup \cdots \cup (\tau_{K_2-1}^-,\tau_{K_2}^+) \cup (\tau_{K_2}^-,\tau_{\mathrm{SN}}),$$

*and unstable for*

$$\tau \in (\tau_0^+,\tau_0^-) \cup \cdots \cup (\tau_{K_2}^+,\tau_{K_2}^-).$$

*(ii) If $\tau_0^+ < \tau_0^- < \cdots < \tau_{n-1}^+ < \tau_n^+ < \tau_{n-1}^-$ for some $2 \le n \le K_2$, then $\tau_0^+ < \tau_0^- < \cdots < \tau_{n-1}^+$ are stability switches of $E_{\tau 2}$. That is, $E_{\tau 2}$ is locally asymptotically stable for*

$$\tau \in [0,\tau_0^+) \cup (\tau_0^-,\tau_1^+) \cup \cdots \cup (\tau_{n-2}^-,\tau_{n-1}^+) \cup (\tau_n^-,\tau_{\mathrm{SN}}),$$

*and unstable for*

$$\tau \in (\tau_0^+,\tau_0^-) \cup \cdots \cup (\tau_{n-1}^+,\tau_n^-).$$

*(iii) If $\tau_0^+ < \tau_1^+ < \tau_0^-$, then system (2.6) undergoes a Hopf bifurcation at $E_{\tau 2}$ for $\tau \in I_2$. Moreover, $E_{\tau 2}$ is locally asymptotically stable for*

$$\tau \in [0,\tau_0^+) \cup (\tau_{K_2}^-,\tau_{\mathrm{SN}}),$$

*and unstable for*

$$\tau \in (\tau_0^+,\tau_{K_2}^-).$$

*(iv) If $\tau_{n+1}^+ = \tau_n^-$ for $n < K_2$, then system (2.6) undergoes a double Hopf bifurcation at $E_{\tau 2}$ when $\tau = \tau_{n+1}^+ = \tau_n^-$.*

When the delay $\tau$ is short, predators track current prey levels closely, so coexistence is self-regulating and stable. As $\tau$ increases, predator recruitment reflects past rather than present prey abundance, creating a timing mismatch that can induce over- or under-compensation and lead to sustained population cycles. Theorem 4.4 shows that this mismatch is not one-directional: as $\tau$ varies, the system alternates between regimes of stable coexistence and regimes of unstable oscillatory dynamics. In ecological terms, delays can create multiple distinct ranges of maturation times that promote recurrent outbreaks, separated by ranges where the same community returns to a steady state of coexistence. This "window" structure emphasizes that the impact of delay depends on its length relative to the intrinsic timescales of the predator-prey interaction, rather than increasing instability monotonically.

**Table 4**
Signs of quantities associated with periodic solutions bifurcating from $E_{\tau 2}$ under the parameter set (4.11).

| $\tau$ | $sign(T_2)$ | $sign(\mu_2)$ | $sign(\beta_2)$ | Figure |
|---|---|---|---|---|
| $\tau_0 \approx 0.01642$ | $> 0$ | $> 0$ | $< 0$ | Fig. 5(D) |
| $\tau_3 \approx 30.66813$ | $< 0$ | $< 0$ | $< 0$ | Fig. 5(G) |

### 4.4. Numerical simulations

#### 4.4.1. Hopf bifurcation

In this section, we perform numerical simulations to investigate the dynamical behaviour of system (2.6) using the MATLAB package DDE-BIFTOOL. The time delay $\tau$ is treated as the bifurcation parameter, while the other parameters are fixed as:

$$b_0 = 1,\ a = 0.2,\ c = 0.3,\ m = 0.5,\ n = 3,\ h = 1.15,\ \delta = 0.02. \tag{4.11}$$

Under these parameter values, system (2.6) satisfies assumptions $(\mathcal{H}_1)$ and $(\mathcal{H}_3)$, and we obtain the critical values:

$$\tau_{TC} \approx 51.3146, \quad \tau_{SN} \approx 51.42, \quad \tau_{\max} \approx 82.5999.$$

According to Theorem 4.3, there are exactly 4 local Hopf bifurcation values with $K_1 = 2$, namely,

$$\tau_0 \approx 0.01642 < \tau_1 \approx 12.39676 < \tau_2 \approx 29.4063 < \tau_3 \approx 30.66813 < \hat{\tau} \approx 30.7179,$$

as illustrated in Fig. 5(A).

There exists a unique positive equilibrium $E_{\tau 2}$ for $\tau \in [0, 51.3146)$, and an additional unstable positive equilibrium $E_{\tau 3}$ appears for $\tau \in (51.3146, 51.42)$ (see Fig. 5(B)).

Clearly, $E_{\tau 2}$ is local asymptotically stable for $\tau \in [0, 0.01642) \cup (30.66813, 51.42]$, and unstable for $\tau \in (0.01642, 30.66813)$. Furthermore, system (2.6) undergoes a Hopf bifurcation at positive $E_{\tau 2}$ as $\tau$ passes through each critical value. Additionally, using the formula provided in Appendix C, the bifurcation properties are summarized in Table 4. In particular, the Hopf bifurcation at $\tau_0$ is supercritical with a stable periodic orbit (see Fig. 5(D)), while the bifurcation at $\tau_3$ is supercritical (see Fig. 5(G)). Furthermore, the system exhibits quasi-periodic behaviour (see Fig. 5(E) and 5(F)).

#### 4.4.2. Global Hopf bifurcation

Under the framework of global Hopf bifurcation theory [32], and using the method similar to that in [25], we can show that system (2.6) does not admit nontrivial periodic solutions of minimal period one. As a result, the same conclusion as Theorem 3.9 in [25] holds:

(C1) All global Hopf branches $\mathbf{C}\left(E_{\tau 2}, \tau_j, \frac{2\pi}{\omega_j \tau_j}\right)$ are bounded for all $1 \le j \le 2K_1 - 2$;

(C2) The two global Hopf branches

$$\mathbf{C}\left(E_{\tau 2}, \tau_j, \frac{2\pi}{\omega_j \tau_j}\right) \quad \text{and} \quad \mathbf{C}\left(E_{\tau 2}, \tau_{2K_1-j-1}, \frac{2\pi}{\omega_{2K_1-j-1}\tau_{2K_1-j-1}}\right)$$

coincide with each other, and thus connect a pair of Hopf bifurcation values $\tau_j$ and $\tau_{2K_1-j-1}$ for $1 \le j \le K_1 - 1$;

(C3) For any $1 \le i, j \le K_1 - 1$, the intersection of global Hopf branches satisfies

$$\mathbf{C}\left(E_{\tau 2}, \tau_i, \frac{2\pi}{\omega_i \tau_i}\right) \cap \mathbf{C}\left(E_{\tau 2}, \tau_j, \frac{2\pi}{\omega_j \tau_j}\right) = \emptyset \text{ if } j \ne 2K_1 - i - 1.$$

The following results are obtained with the parameter values given in (4.11). Fig. 6(A) shows the global Hopf branches $\mathbf{C}\left(E_{\tau 2}, \tau_j, \frac{2\pi}{\omega_j \tau_j}\right)$ bifurcating from the equilibrium $E_{\tau 2}$ near each bifurcation point $\tau_j$ for $0 \le j \le 3$. It is observed that the first and fourth branches (corresponding to $\tau_0$ and $\tau_3$) are unbounded and connected, while the second and third branches (corresponding to $\tau_1$ and $\tau_2$) are bounded and connected.

The stability of the bifurcated periodic solutions is determined by the associated principal Floquet multiplier. As shown in Fig. 6(B), if the principal Floquet multiplier exceeds 1, the periodic solution is unstable; otherwise, it is stable.

#### 4.4.3. Stability switches

To numerically investigate the potential stability switches of $E_{\tau 2}$ when $(\mathcal{H}_1)$ and $(\mathcal{H}_4)$ hold, we consider a new set of parameters

$$b_0 = 1,\ a = 0.5,\ c = 8,\ m = 4.1,\ n = 12,\ h = 0.5666. \tag{4.12}$$

We present four numerical scenarios by varying the value of $\delta$, as outlined in **Scenatio 1-4**, to validate the results in Theorem 4.4.

**Scenario 1:** By setting $\delta = 0.008$, we obtain $\widetilde{\tau} \approx 6.7175$. There are exactly four Hopf bifurcation values:

$$\tau_0^+ \approx 0.0105 < \tau_0^- \approx 2.3656 < \tau_{11}^+ \approx 5.9432 < \tau_{12}^+ \approx 6.6203 < \widetilde{\tau},$$

as shown in Fig. 7(A). Moreover, $E_{\tau 2}$ is locally asymptotically stable for $\tau \in [0, \tau_0^+) \cup (\tau_0^-, \tau_{11}^+) \cup (\tau_{12}^+, \tau_{SN})$, and unstable for $\tau \in (\tau_0^+, \tau_0^-) \cup (\tau_{11}^+, \tau_{12}^+)$ (see Fig. 7(E)).

**Scenario 2:** By setting $\delta = 0.006$, we obtain $\widetilde{\tau} \approx 8.9567$. There are exactly four Hopf bifurcation values:

$$\tau_0^+ \approx 0.0105 < \tau_0^- \approx 2.7569 < \tau_1^+ \approx 5.2375 < \tau_1^- \approx 8.3941 < \widetilde{\tau},$$

as shown in Fig. 7(B). Moreover, $E_{\tau 2}$ is locally asymptotically stable for $\tau \in [0, \tau_0^+) \cup (\tau_0^-, \tau_1^+) \cup (\tau_1^-, \tau_{SN})$, and unstable for $\tau \in (\tau_0^+, \tau_0^-) \cup (\tau_1^+, \tau_1^-)$ (see Fig. 7(F)).

**Scenario 3:** By setting $\delta = 0.003$, we obtain $\widetilde{\tau} \approx 17.9133$. There are exactly six Hopf bifurcation values:

$$\begin{aligned}\tau_0^+ \approx 0.0104 < \tau_0^- \approx 3.9358 < \tau_1^+ \approx 4.8572 < \tau_2^+ \approx 10.4020 \\ < \tau_1^- \approx 11.8027 < \tau_2^- \approx 16.6 < \widetilde{\tau},\end{aligned}$$

as shown in Fig. 7(C). Moreover, $E_{\tau 2}$ is locally asymptotically stable for $\tau \in [0, \tau_0^+) \cup (\tau_0^-, \tau_1^+) \cup (\tau_2^-, \tau_{SN})$, and unstable for $\tau \in (\tau_0^+, \tau_0^-) \cup (\tau_1^+, \tau_2^-)$ (see Fig. 7(G)).

**Scenario 4:** By setting $\delta = 0.0019$, we obtain $\widetilde{\tau} \approx 28.2842$. There are exactly eight Hopf bifurcation values:

$$\begin{aligned}\tau_0^+ \approx 0.0104 < \tau_1^+ \approx 4.7627 < \tau_0^- \approx 4.9334 < \tau_2^+ \approx 9.8356 \\ < \tau_1^- \approx 14.3175 < \tau_3^+ \approx 15.4250 \\ < \tau_2^- \approx 20.7824 < \tau_4^+ \approx 22.2341 < \tau_3^- \approx 25.501 < \tau_4^- \approx 28.2317 \\ < \widetilde{\tau},\end{aligned}$$

as shown in Fig. 7(D). Moreover, $E_{\tau 2}$ is locally asymptotically stable for $\tau \in [0, \tau_0^+) \cup (\tau_4^-, \tau_{SN})$, and unstable for $\tau \in (\tau_0^+, \tau_4^-)$ (see Fig. 7(H)).

#### 4.4.4. Sensitivity analysis

We apply the Partial Rank Correlation Coefficient (PRCC) method to conduct a global sensitivity analysis, quantifying the relative influence of the model parameters on the long-term dynamics of the prey ($u$) and predator ($v$) populations governed by system (2.6). Here we focus on the personality-related parameters ($a$, $b_0$, $c$, $h$) and the time delay $\tau$. Results are provided in Fig. 8.

For the prey population $u$, the intrinsic predation rate $b_0$ exhibits a strong negative effect, whereas the handling time $h$ has a high positive effect. The time delay $\tau$ has a moderate positive association, consistent with the interpretation that longer delays can temporarily relieve predation pressure before newly matured predators enter the predation pool. For the predator population $v$, PRCC magnitudes are generally smaller than for $u$, as expected from trophic conversion and predator losses. The parameter $a$, which is linked to predator-dependent predation, shows the strongest negative influence, suggesting that certain behavioral responses captured by an increased $a$ are detrimental to the predator density in the long run. In contrast, $b_0$ is the main positive driver of $v$. Notably, $\tau$ also ranks among the second strongest negative contributors to $v$, emphasizing the importance of incorporating time delay to capture the regulatory mechanisms in this predator-prey system.

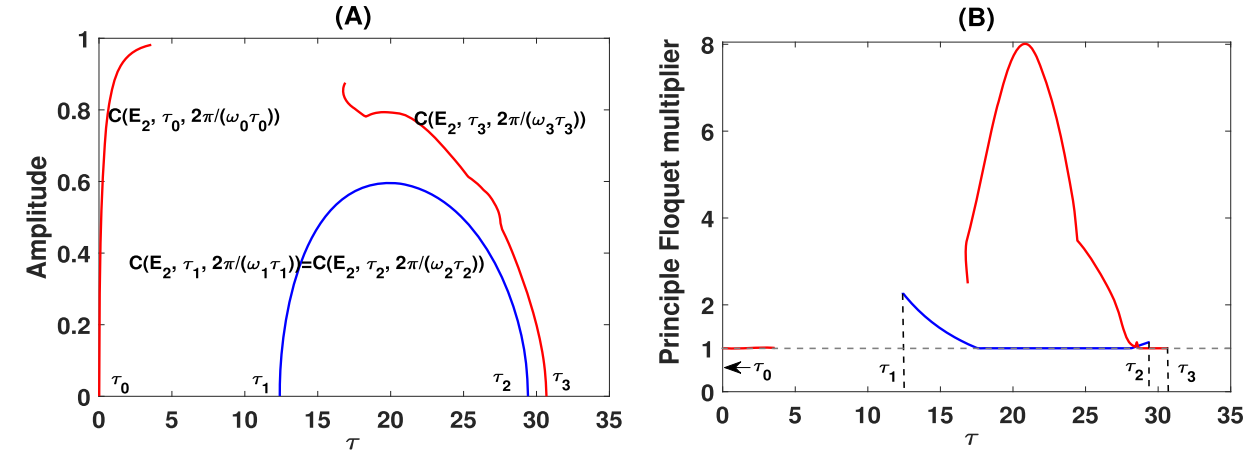


**Fig. 6.** (A) Global Hopf branches of system (2.6) with parameters from (4.11). (B) Corresponding principal Floquet multipliers of periodic solutions.

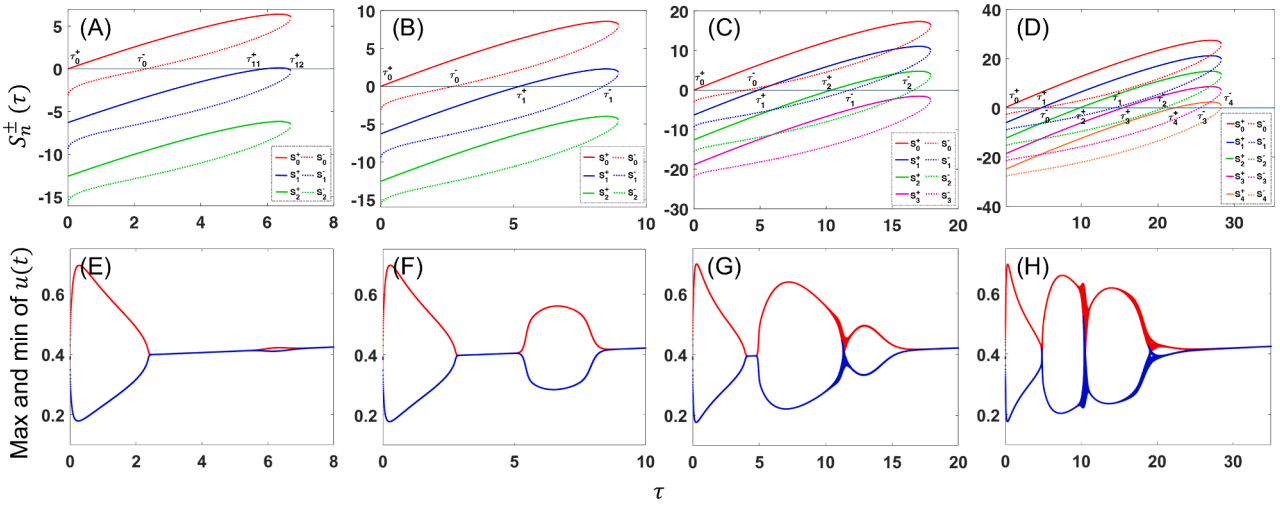


**Fig. 7.** (A)-(D) Plots of the functions $S_n^{\pm}(\tau)$, where solid curves represent $S_n^{+}(\tau)$ and dashed curves represent $S_n^{-}(\tau)$. (E)-(H) Bifurcation diagrams showing the maximum (red) and minimum (blue) values of $u(t)$ as $\tau$ varies. All other parameter choices are described in (4.12).

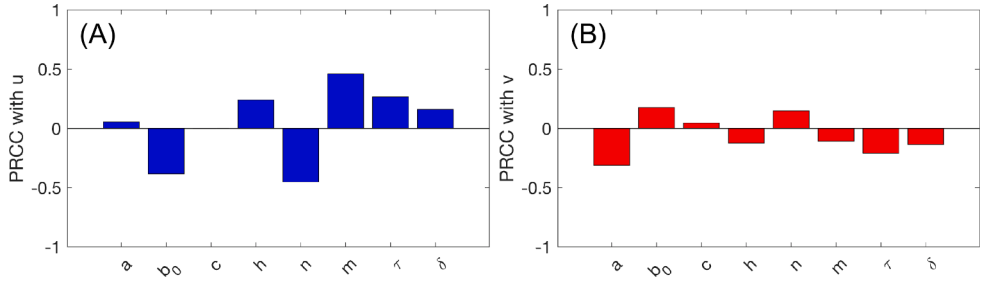


**Fig. 8.** Global sensitivity analysis of system (2.6).

## 5. Discussion

We extended the Rosenzweig-MacArthur framework by coupling a nonlinear, personality-dependent attack rate with a maturation delay in predator growth. The former captures within-population behavioural heterogeneity (bold-shy types modulating encounter and attack rates), while the latter results from a stage-structured derivation that introduces a fixed developmental time. Taken together, these mechanisms yield a biologically richer predation model suitable for systematic study of species interactions and their regulation.

For the instantaneous system ($\tau = 0$), we established well-posedness and gave a complete local classification of equilibria: total extinction ($E_0$), prey-only persistence ($E_1$), and up to two coexistence points ($E_2, E_3$). The coexistence point $E_3$ is always unstable; $E_2$ changes stability with parameters and is therefore the key organizing state. By varying the harvesting parameter $h$, we rigorously verified (analytically and numerically) the occurrence of transcritical, Hopf, and saddle-node bifurcations, as well as codimension-two cusp and Bogdanov-Takens (BT) points (Fig. 4). Global structures, homoclinic loops and saddle-node bifurcations of limit cycles, were also detected. These features generate bistability between boundary and interior states, implying that the long-term outcome (extinction, prey-only, or coexistence) can depend sensitively on initial densities.

We identified three BT bifurcations associated with the parameter pairs $(n, m)$, $(a, m)$, and $(a, c)$. In their neighbourhoods, homoclinic orbits and folds of cycles appear, mediating transitions between stable coexistence and oscillations. This geometry organizes the local one-parameter bifurcations and explains rapid qualitative shifts when parameters cross narrow thresholds.

Introducing maturation ($\tau > 0$) through the juvenile-survival factor $e^{-\delta\tau}$ qualitatively reshapes the picture in ecologically intuitive ways: small increases in developmental time can destabilize steady coexistence and generate sustained oscillations, consistent with classic delay effects [23]. Continuing in $\tau$ from the stable instantaneous regime, we derived conditions for persistence of stability, located Hopf thresholds where a complex conjugate pair crosses the imaginary axis, and characterized stability switching when two frequency branches coexist. Specifically,

(1) If $(\mathcal{H}_1)$ and $(\mathcal{H}_2)$ hold, all eigenvalues remain in the left half-plane for all $\tau \geq 0$, and the coexistence equilibrium $E_{\tau 2}$ stays stable.
(2) Under $(\mathcal{H}_1)$ and $(\mathcal{H}_3)$, a Hopf bifurcation occurs at $\tau = \tau_c$, producing a family of periodic solutions. Time series and continuation reveal periodic and quasi-periodic behaviour (Fig. 5) and global Hopf branches that connect critical delays (Fig. 6).
(3) If $(\mathcal{H}_1)$ and $(\mathcal{H}_4)$ hold, two frequency branches appear, enabling multiple stability switches (Fig. 7). We observe three subcases: (i) at least three switches; (ii) two switches; and (iii) a single switch.

Hence, maturation delay alone can create rich oscillatory dynamics, bistability, and complicated bifurcation structures, even without additional nonlinearities.

Because $h$ and the composite survival factor $e^{-\delta\tau}$ directly or indirectly regulate the location and stability of equilibria and cycles, harvest intensity and juvenile survival act as levers for system behaviour. Our results indicate that carefully regulating $h$ can avoid undesirable transitions (e.g., from steady coexistence to large-amplitude cycles) and that increases in juvenile mortality $\delta$ (or effective development time $\tau$) can either stabilize or destabilize dynamics depending on where the system sits relative to Hopf and BT loci. These insights suggest management strategies that prioritize (i) constraining $h$ away from transcritical/saddle-node thresholds and (ii) targeting juvenile stages when the system is close to delay-induced Hopf boundaries.

Parameter values in simulations are representative rather than directly empirical; nonetheless, the mechanisms we analyse are structural and thus broadly informative. Natural next steps include: (i) spatial extensions (reaction-diffusion or patch models) with memory-driven movement; (ii) stochastic formulations to quantify extinction risk near global bifurcations; and (iii) data-assimilation studies to estimate personality effects on functional-response parameters and to validate delay-induced oscillations in the field.

In summary, coupling personality-dependent foraging with maturation delay refines theory for predator-prey systems by revealing how behavioural heterogeneity and ontogenetic timing interact to generate oscillations, multistability, and intricate bifurcation geometry. This coupling yields concrete, testable thresholds, in biologically interpretable parameter combinations, for when coexistence is stable, when cycles emerge, and when management interventions are most effective.

## CRediT authorship contribution statement

**Heping Jiang:** Writing – review & editing, Writing – original draft, Visualization, Methodology, Investigation, Formal analysis, Conceptualization; **Shan Gao:** Writing – review & editing, Visualization, Validation; **Hao Wang:** Writing – review & editing, Validation, Supervision, Software, Project administration, Methodology, Conceptualization.

## Data availability

Data sharing is not applicable to this article as no datasets were generated or analyzed during the current study

## Declaration of competing interest

The authors declare that they have no known competing financial interests or personal relationships that could have appeared to influence the work reported in this paper.

## Acknowledgments

Heping Jiang gratefully acknowledges support from the young Backbone Teachers Overseas Study and Research Funding Project in Department of Education in Anhui Province
(No.JWFX2023035). Hao Wang gratefully acknowledges support from the Natural Sciences and Engineering Research Council of Canada (Individual Discovery Grant RGPIN-2025-05734) and the Canada Research Chairs program (Tier 1 Canada Research Chair Award).

## Appendix A. The stability of the bifurcating limit cycle for system (2.5)

In this section, we will discuss the stability behaviour of the bifurcating periodic solutions and the direction of generated limit cycle by using the normal form theory and computing the first Lyapunov number. Firstly, let us choose the transformation $z_1 = u - u_2$ and $z_2 = v - v_2$, which shift the equilibrium $E_2(u_2, v_2)$ into origin. After incorporating this transformation into system (2.5), we get

$$\begin{cases} \frac{dz_1}{dt} = (z_1 + u_2)\big(1 - (z_1 + u_2)\big) - \frac{\beta(z_1+u_2, z_2+v_2)(z_1+u_2)(z_2+v_2)}{1+\beta(z_1+u_2, z_2+v_2)h(z_1+u_2)}, \\ \frac{dz_2}{dt} = n\frac{\beta(z_1+u_2, z_2+v_2)(z_1+u_2)(z_2+v_2)}{1+\beta(z_1+u_2, z_2+v_2)h(z_1+u_2)} - m\big(z_2 + v_2\big), \end{cases}$$

expanding in Taylor's series about $(z_1, z_2) = (0, 0)$ up to the third order term, we obtained the following system:

$$\begin{cases} \dot{z_1} = \sum_{i+j=1}^{3} a_{ij} z_1^i z_2^j + O_1\big(|z_1, z_2|^4\big), \\ \dot{z_2} = \sum_{i+j=1}^{3} b_{ij} z_1^i z_2^j + O_2\big(|z_1, z_2|^4\big), \end{cases} \tag{A.1}$$

where terms $a_{ij}$ and $b_{ij}$, $i, j = 0, 1, 2, 3, i + j \leq 3$ are the coefficients of the power series expansions of $f(x, y)$ and $g(x, y)$ at $E_2(u_2, v_2)$, $O_k\big(|z_1, z_2|^4\big)$, $k = 1, 2$ are the same order infinity.

The system described above (A.1) may be represented as:

$$\dot{Z} = J\big(E_2\big)Z + A(Z), \tag{A.2}$$

where $Z = \big(z_1 \ z_2\big)^T$ and

$$A = \begin{pmatrix} A_1 \\ A_2 \end{pmatrix} = \begin{pmatrix} \sum_{i+j=2}^{3} a_{ij} z_1^i z_2^j \\ \sum_{i+j=2}^{3} b_{ij} z_1^i z_2^j \end{pmatrix}.$$

It is easy to verify that $V = (a_{01} \quad i\omega_0 - a_{10})^T$ is an eigenvector of the Jacobian matrix $J(E^*)$ corresponding to the eigenvalue $i\omega_0$ when $h = h_{HB}$.

Let us define

$$S = (Re(V), Im(V)) = \begin{pmatrix} a_{10} & 0 \\ -a_{01} & i\omega_0 \end{pmatrix},$$

choose $Z = SX$ or $X = S^{-1}Z$, where $X = (x_1 \ \ x_2)^T$, through this transformation the system (A.2) may be written as:

$$\dot{X} = \big(S^{-1}J(E)S\big)X + S^{-1}A(SX).$$

This can be represented as

$$\begin{pmatrix} \dot{x}_1 \\ \dot{x}_2 \end{pmatrix} = \begin{pmatrix} 0 & -\omega_0 \\ \omega_0 & 0 \end{pmatrix}\begin{pmatrix} x_1 \\ x_2 \end{pmatrix} + \begin{pmatrix} M^1(x_1, x_2; h = h_{HB}) \\ M^2(x_1, x_2; h = h_{HB}) \end{pmatrix}, \tag{A.3}$$

where $M^1$ and $M^2$ are given by

$$M^1\big(x_1, x_2; h = h_{HB}\big) = \frac{A_1}{a_{01}},$$

$$M^2(x_1,x_2;h=h_{HB})=-\frac{a_{10}A_1+a_{01}A_2}{a_{01}\omega_0},$$

with

$$\begin{aligned}A_1=&\left(a_{02}a_{01}^2-a_{11}a_{01}a_{10}+a_{02}a_{10}^2\right)x_1^2+\omega_0\left(2a_{02}a_{10}-a_{11}a_{01}\right)x_1x_2\\&+\omega_0^2a_{02}x_2^2\\&+\left(a_{30}a_{01}^3+a_{12}a_{01}a_{10}^2-a_{21}a_{01}^2a_{10}-a_{03}a_{10}^3\right)x_1^3\\&+\omega_0\left(2a_{12}a_{10}a_{01}-a_{21}a_{01}^2-3a_{03}a_{10}^2\right)x_1^2x_2+\omega_0^2\left(a_{12}a_{01}-3a_{03}a_{10}\right)\\&x_1x_2^2-\omega_0^3a_{03}x_2^3,\end{aligned}$$

and

$$\begin{aligned}A_2=&\left(b_{02}a_{01}^2-b_{11}a_{01}a_{10}+b_{02}a_{10}^2\right)x_1^2+\omega_0\left(2b_{02}a_{10}-b_{11}a_{01}\right)x_1x_2\\&+\omega_0^2b_{02}x_2^2\\&+\left(b_{30}a_{01}^3+b_{12}a_{01}a_{10}^2-b_{21}a_{01}^2a_{10}-b_{03}a_{10}^3\right)x_1^3\\&+\omega_0\left(2b_{12}a_{10}a_{01}-b_{21}a_{01}^2-3b_{03}a_{10}^2\right)x_1^2x_2+\omega_0^2\left(b_{12}a_{01}-3b_{03}a_{10}\right)\\&x_1x_2^2-\omega_0^3b_{03}x_2^3.\end{aligned}$$

Now, to observe the stability behaviour of the periodic solutions here, we will compute the first Lyapunov number based on the normal form (A.3) as:

$$\begin{aligned}L=&\frac{1}{16}\left[M_{111}^1+M_{122}^1+M_{112}^2+M_{222}^2\right]\\&+\frac{1}{16\omega_0}\left[M_{12}^1\left(M_{11}^1+M_{22}^1\right)-M_{12}^2\left(M_{11}^2+M_{22}^2\right)-M_{11}^1M_{11}^2+M_{22}^1M_{22}^2\right],\end{aligned}$$

where

$$M_{ij}^k=\frac{\partial^2M^k}{\partial x_i\partial x_j}|_{(x_1,x_2;h)=(0,0;h_{HB})},\quad M_{ijl}^k=\frac{\partial^3M^k}{\partial x_i\partial x_j\partial x_l}|_{(x_1,x_2;h)=(0,0;h_{HB})},$$

for $i,j,k,l\in1,2$. Now, we can observe that if $L<0$, then supercritical Hopf bifurcation occurs, and a stable limit cycle will be created around the interior equilibrium point $E_2(u_2,v_2)$, whereas if $L>0$, then subcritical Hopf bifurcation occurs, and an unstable limit cycle will be created around the interior equilibrium point $E_2(u_2,v_2)$.

## Appendix B. The local bifurcation curves are are derived and expressed

Let

$$\begin{cases}u=u_1,\\ v=a_1+a_2u_1+a_3v_1+a_4u_1^2+a_5u_1v_1+a_6v_1^2+P_1(u_1,v_1,\varepsilon_1,\varepsilon_2),\end{cases}$$

then system (3.9) can be written as

$$\begin{cases}\frac{du}{dt}=v,\\ \frac{dv}{dt}=c_1+c_2u+c_3v+c_4u^2+c_5uv+c_6v^2+Q_2(u,v,\varepsilon_1,\varepsilon_2),\end{cases}\tag{B.1}$$

where $Q_2(u,v,\varepsilon_1,\varepsilon_2)$ are $C^\infty$ function at least of third order with respect to $(u,v)$, whose coefficients depend smoothly on $\varepsilon_1$ and $\varepsilon_2$, and

$$c_1=a_3b_1,\ c_2=\frac{a_3^2-a_2a_3b_3+a_3a_5b_1-2a_2a_6b_1}{a_3},\ c_3=\frac{a_2a_3+a_3b_3+2a_6b_1}{a_3},$$

$$\begin{aligned}c_4=&\frac{a_2^2(a_6(a_2+2b_3)-a_3(a_5+b_6))+a_3^2(a_3b_4-a_4b_3+a_5b_2)}{a_3^2}\\&-\frac{a_2a_3(a_4b_5+2a_6b_2+a_5b_3)+2a_3a_4a_6b_1}{a_3^2},\end{aligned}$$

$$c_5=\frac{-2a_2^2a_6+2a_3^2a_4+a_3^2a_5+a_3a_5b_3-4a_2a_6b_3}{a_3^2},$$

$$c_6=\frac{a_2a_6+a_3a_5+a_3b_6+2a_6b_3}{a_3^2}.$$

Next, introduce a new time variable $s$ by $dt=(1-c_6u)ds$. Renaming $s$ as $t$. system (B.1) becomes

$$\begin{cases}\frac{du}{dt}=(1-c_6u)v,\\ \frac{dv}{dt}=(1-c_6u)\left(c_1+c_2u+c_3v+c_4u^2+c_5uv+c_6v^2+Q_2(u,v,\varepsilon_1,\varepsilon_2)\right).\end{cases}\tag{B.2}$$

Let $u_1=u,v_1=v(1-c_6u)$, then (B.2) can be rewritten as

$$\begin{cases}\frac{du_1}{dt}=v_1,\\ \frac{dv_1}{dt}=d_1+d_2u_1+d_3v_1+d_4u_1^2+d_5u_1v_1+Q_3(u_1,v_1,\varepsilon_1,\varepsilon_2),\end{cases}$$

where $Q_3(u_1,v_1,\varepsilon_1,\varepsilon_2)$ are $C^\infty$ function at least of third order with respect to $(u_1,v_1)$, whose coefficients depend smoothly on $\varepsilon_1$ and $\varepsilon_2$, and

$$d_1=c_1,\ d_2=c_2-2c_1c_6,\ d_3=c_3,\ d_4=c_4-2c_2c_6+c_1c_6^2,\ d_5=c_5-c_3c_6.$$

Next, we continue to make the following two transformations successively

$$u=u_1+\frac{d_2}{2d_4},\quad v=v_1,$$

$$u_1=\frac{e_4^2}{e_3}u,\quad v_1=\frac{e_4^3}{e_3^2}v,\quad s=\frac{e_3}{e_4}t,$$

then we finally obtain (still denote $u_1,v_1,s$ by $u,v,t$, respectively)

$$\begin{cases}\frac{du}{dt}=v,\\ \frac{dv}{dt}=\mu_1+\mu_2v+u^2+uv+Q_4(u,v,\varepsilon_1,\varepsilon_2),\end{cases}$$

where $Q_4(u,v,\varepsilon_1,\varepsilon_2)$ are $C^\infty$ function at least third order with respect to $(u,v)$, whose coefficients depend smoothly on $\varepsilon_1$ and $\varepsilon_2$, and

$$\mu_1=\frac{e_1e_4^4}{e_3^3},\quad \mu_2=\frac{e_2e_4}{e_3}.$$

We are only interested in the phase portraits of system (2.5) when $u$ and $v$ lies in a small neighborhood of the interior equilibrium $E_*(u_*,v_*)$. By the results of Perko [30], the local bifurcation curves are expressed as follows:

(1) The saddle-node bifurcation curve is $SN=\{(\mu_1,\mu_2)|\mu_1=0,\mu_2\neq0\}$;
(2) The Hopf bifurcation curve is $H=\left\{(\mu_1,\mu_2)|\mu_2=-\sqrt{-\mu_1},\mu_1<0\right\}$;
(3) The homoclinic bifurcation curve is $HL=\left\{(\mu_1,\mu_2)|\mu_2=-\frac{5}{7}\sqrt{-\mu_1},\mu_1<0\right\}$.

## Appendix C. Stability and direction of the Hopf bifurcation for system (2.6)

In the Section 4.3.1 , we have already obtained some sufficient conditions ensuring that system (2.6) undergoes a Hopf bifurcation at $E_{\tau2}(u_{\tau2},v_{\tau2})$. In this section, we shall use the center manifold and normal form theories theories presented by Hasssard et al. [33] to study the direction of Hopf bifurcation and the stability of Hopf bifurcating periodic solutions from $E_{\tau2}(u_{\tau2},v_{\tau2})$ under the conditions of Theorem 4.4. Without loss of generality, we let $\tau^*$ be the critical value of at which system (2.6) undergoes a Hopf bifurcation at $E_{\tau2}(u_{\tau2},v_{\tau2})$. Setting $\tau=\tau^*+\mu$, then $\mu=0$ is Hopf bifurcation value of system (2.6).

Let $\tilde{u}(t)=u(t)+u_{\tau2},\tilde{v}(t)=v(t)+v_{\tau2}$, and still denote $(\tilde{u}(t),\tilde{v}(t))$ by $(u(t),v(t))$, and by rescalling the time $t\to(t/\tau)$, system (2.6) can be writen in the form

$$\begin{pmatrix}\dot{u}(t)\\ \dot{v}(t)\end{pmatrix}=\tau M_1\begin{pmatrix}u(t)\\ v(t)\end{pmatrix}+\tau N_1\begin{pmatrix}u(t-1)\\ u(t-1)\end{pmatrix}+\tau F(u,v),$$

where

$$M_1 = \begin{pmatrix} a_1(\tau) & a_2(\tau) \\ 0 & b_3(\tau) \end{pmatrix}, \quad N_1 = \begin{pmatrix} 0 & 0 \\ b_1(\tau) & b_2(\tau) \end{pmatrix},$$

and

$$F(u,v) = \begin{pmatrix} f(u(t),v(t)) \\ g(u(t-1),v(t-1)) \end{pmatrix}$$
$$= \begin{pmatrix} \frac{f_{20}}{2}u^2(t) + f_{11}u(t)v(t) + \frac{f_{02}}{2}v^2(t) + \frac{f_{30}}{6}u^3(t) + \cdots \\ \frac{g_{20}}{2}u^2(t-1) + g_{11}u(t-1)v(t-1) + \frac{g_{02}}{2}v^2(t-1) + \frac{g_{30}}{6}u^3(t-1) + \cdots \end{pmatrix},$$

with

$$a_1(\tau) = 1 - 2u_{\tau 2} - A_1(u_{\tau 2}, v_{\tau 2}), \quad a_2(\tau) = -A_2(u_{\tau 2}, v_{\tau 2}),$$
$$b_1(\tau) = ne^{-\delta\tau}A_1(u_{\tau 2}, v_{\tau 2}), \quad b_2(\tau) = ne^{-\delta\tau}A_2(u_{\tau 2}, v_{\tau 2}), \quad b_3(\tau) = -m.$$

It is not difficult to verity that the vector $q(\theta) = \left(q_1,\ q_2\right)^T e^{i\omega^*\tau^*\theta}(\theta \in [-1,0])$ and $q^*(s) = \frac{1}{D}\left(q_1^*,\ q_2^*\right)^T e^{i\omega^*\tau^* s}(s \in [0,1])$ are the eigenvector of the linearized operator of the abstract ordinary equations associated with system (2.6) and it's adjoint operator corresponding to eigenvalue $i\omega^*\tau^*$ and $-i\omega^*\tau^*$, respectively, where

$$q_1 = q_1^* = 1, \quad q_2 = \frac{i\omega^* - a_1(\tau)}{a_2(\tau)}, \quad q_2^* = \frac{-i\omega^* - a_1(\tau)}{b_1(\tau)e^{i\omega^*\tau^*}},$$

and

$$D = 1 + \overline{q}_2^* q_2 + \tau^*\left(b_1(\tau)\overline{q}_2^* + b_2(\tau)\overline{q}_2^* q_2\right)e^{-i\omega^*\tau^*}$$
$$= 1 + \tau^*(i\omega^* - a_1(\tau)) + \frac{\left(i\omega^* - a_1(\tau)\right)^2}{a_2(\tau)b_1(\tau)}\left(e^{i\omega^*\tau^*} + b_2(\tau)\tau^*\right).$$

Hence, we obtain the coefficients determining the important quantities:

$$\mathfrak{g}_{20} = \frac{\tau^*}{D}\left[\overline{q}_1^*\left(f_{20}q_1^2 + 2f_{11}q_1q_2 + f_{02}q_2^2\right) + \overline{q}_2^*\left(g_{20}q_1^2 + 2g_{11}q_1q_2 + g_{02}q_2^2\right)e^{-2i\omega^*\tau^*}\right],$$
$$\mathfrak{g}_{11} = \frac{\tau^*}{D}\left[\overline{q}_1^*\left(f_{20}|q_1|^2 + f_{11}\left(q_1\overline{q}_2 + \overline{q}_1q_2\right) + f_{02}|q_2|^2\right)\right.$$
$$\left.+\overline{q}_2^*\left(g_{20}|q_1|^2 + g_{11}\left(q_1\overline{q}_2 + \overline{q}_1q_2\right) + g_{02}|q_2|^2\right)\right],$$
$$\mathfrak{g}_{02} = \frac{\tau^*}{D}\left[\overline{q}_1^*\left(f_{20}\overline{q}_1^2 + 2f_{11}\overline{q}_1\overline{q}_2 + f_{02}\overline{q}_2^2\right) + \overline{q}_2^*\left(g_{20}\overline{q}_1^2 + 2g_{11}\overline{q}_1\overline{q}_2 + g_{02}\overline{q}_2^2\right)e^{2i\omega^*\tau^*}\right],$$
$$\mathfrak{g}_{21} = \frac{\tau^*}{D}\left\{\overline{q}_1^*\left[f_{20}\left(W_{20}^{(1)}(0)\overline{q}_1 + 2W_{11}^{(1)}(0)q_1\right) + f_{02}\left(W_{20}^{(2)}(0)\overline{q}_2 + 2W_{11}^{(2)}(0)q_2\right)\right.\right.$$
$$+f_{11}\left(W_{20}^{(1)}(0)\overline{q}_2 + 2W_{11}^{(1)}(0)q_2 + W_{20}^{(2)}(0)\overline{q}_1 + 2W_{11}^{(2)}(0)q_1\right)$$
$$\left.+f_{30}q_1^2\overline{q}_1 + f_{21}\left(q_1^2\overline{q}_2 + 2|q_1|^2q_2\right) + f_{12}\left(q_2^2\overline{q}_1 + 2|q_2|^2q_1\right) + f_{03}q_2^2\overline{q}_2\right]$$
$$+\overline{q}_2^*\left[g_{20}\left(W_{20}^{(1)}(-1)\overline{q}_1e^{i\omega^*\tau^*} + 2W_{11}^{(1)}q_1e^{-i\omega^*\tau^*}\right)\right.$$
$$+g_{02}\left(W_{20}^{(2)}(-1)\overline{q}_2e^{i\omega^*\tau^*} + 2W_{11}^{(2)}(-1)q_2e^{-i\omega^*\tau^*}\right)$$
$$+g_{11}\left(W_{20}^{(1)}(-1)\overline{q}_2e^{i\omega^*\tau^*} + 2W_{11}^{(1)}(-1)q_2e^{-i\omega^*\tau^*}\right.$$
$$\left.+W_{20}^{(2)}(-1)\overline{q}_1e^{i\omega^*\tau^*} + 2W_{11}^{(2)}(-1)q_1e^{-i\omega^*\tau^*}\right)$$
$$\left.\left.+\left(g_{30}q_1^2\overline{q}_1 + g_{21}\left(q_1^2\overline{q}_2 + 2|q_1|^2q_2\right) + g_{12}\left(q_2^2\overline{q}_1 + 2|q_2|^2q_1\right) + g_{03}q_2^2\overline{q}_2\right)e^{-i\omega^*\tau^*}\right]\right\},$$

where

$$W_{20}(\theta) = \frac{i\mathfrak{g}_{20}}{\omega^*\tau^*}q(0)e^{i\omega^*\tau^*\theta} + \frac{i\overline{\mathfrak{g}}_{02}}{3\omega^*\tau^*}\overline{q}(0)e^{-i\omega^*\tau^*\theta} + \widehat{E}_1e^{2i\omega^*\tau^*\theta},$$
$$W_{11}(\theta) = -\frac{i\mathfrak{g}_{11}}{\omega^*\tau^*}q(0)e^{i\omega^*\tau^*\theta} + \frac{i\overline{\mathfrak{g}}_{11}}{\omega^*\tau^*}\overline{q}(0)e^{-i\omega^*\tau^*\theta} + \widehat{E}_2,$$

and

$$\widehat{E}_1 = 2\begin{pmatrix} 2i\omega^* - a_1(\tau) & -a_2(\tau) \\ -b_1(\tau)e^{-2i\omega^*\tau^*} & 2i\omega^* - b_2(\tau)e^{-2i\omega^*\tau^*} - b_3(\tau) \end{pmatrix}^{-1}$$
$$\times\begin{pmatrix} \frac{1}{2}f_{20}q_1^2 + f_{11}q_1q_2 + \frac{1}{2}f_{02}q_2^2 \\ \frac{1}{2}g_{20}q_1^2 + g_{11}q_1q_2 + \frac{1}{2}g_{02}q_2^2 \end{pmatrix},$$
$$\widehat{E}_2 = -\begin{pmatrix} a_1(\tau) & a_2(\tau) \\ b_1(\tau) & b_2(\tau) + b_3(\tau) \end{pmatrix}^{-1}$$
$$\times\begin{pmatrix} \frac{1}{2}f_{20}|q_1|^2 + f_{11}(q_1\overline{q}_2 + \overline{q}_1q_2) + \frac{1}{2}f_{02}|q_2|^2 \\ \frac{1}{2}g_{20}|q_1|^2 + g_{11}(q_1\overline{q}_2 + \overline{q}_1q_2) + \frac{1}{2}g_{02}|q_2|^2 \end{pmatrix}.$$

Consequently, we can compute the following values:

$$c_1(0) = \frac{i}{2\omega^*\tau^*}\left(\mathfrak{g}_{11}\mathfrak{g}_{20} - 2|\mathfrak{g}_{11}|^2 - \frac{|\mathfrak{g}_{02}|^2}{3}\right) + \frac{\mathfrak{g}_{21}}{2},$$
$$\mu_2 = -\frac{Re(c_1(0))}{Re(\lambda'(\tau^*))}, \quad \beta_2 = 2Re(c_1(0)), \quad T_2 = -\frac{Im(c_1(0)) + \mu_2 Im(\lambda'(\tau^*))}{\omega^*\tau^*},$$

which determine the properties of bifurcating periodic solution at the critical value $\tau^*$. To be concrete, $\mu_2$ determines the direction of the Hopf bifurcation: If $\mu_2 > 0 (resp. < 0)$, then Hopf bifurcation are forward (resp. backward); $\beta_2$ determines the stability of bifurcating periodic solutions: The bifurcating periodic solutions on the center manifold are stable (resp. unstable) if $\beta_2 < 0 (resp. > 0)$; $T_2$ determines the periods of the bifurcating periodic solutions: The periods increase (resp. decrease) if $T_2 > 0 (resp. < 0)$.

## References


[1] D.J. Hall, S.T. Threlkeld, C.W. Burns, P.H. Crowley, The size-efficiency hypothesis and the size structure of zooplankton communities, Annu. Rev. Ecol. Syst. (1976) 177–208.
[2] Y. Ishii, M. Shimada, The effect of learning and search images on predator–prey interactions, Popul. Ecol. 52 (1) (2010) 27–35.
[3] B.L. Peckarsky, C.A. Cowan, M.A. Penton, C. Anderson, Sublethal consequences of stream-dwelling predatory stoneflies on mayfly growth and fecundity, Ecology 74 (6) (1993) 1836–1846.
[4] D.K. Skelly, Activity level and the susceptibility of anuran larvae to predation, Anim. Behav. 47 (2) (1994) 465–468.
[5] E.E. Werner, J.F. Gilliam, D.J. Hall, G.G. Mittelbach, An experimental test of the effects of predation risk on habitat use in fish, Ecology 64 (6) (1983) 1540–1548.
[6] T. Yoshida, L.E. Jones, S.P. Ellner, G.F. Fussmann, N.G. Hairston, Jr, Rapid evolution drives ecological dynamics in a predator–prey system, Nature 424 (6946) (2003) 303–306.
[7] C.S. Holling, Some characteristics of simple types of predation and parasitism1, Can. Entomol. 91 (7) (1959) 385–398.
[8] A.J. Lotka, Undamped oscillations derived from the law of mass action, J. Am. Chem. Soc. 42 (8) (1920) 1595–1599.
[9] M.L. Rosenzweig, R.H. MacArthur, Graphical representation and stability conditions of predator-prey interactions, Am. Nat. 97 (895) (1963) 209–223.
[10] V. Volterra, Variazioni e Fluttuazioni Del Numero d'individui in Specie Animali Conviventi, Società anonima Tipografica" Leonardo da Vinci", 1926.
[11] D.I. Bolnick, P. Amarasekare, M.S. Araújo, R. Bürger, J.M. Levine, M. Novak, V.H.W. Rudolf, S.J. Schreiber, M.C. Urban, D.A. Vasseur, Why intraspecific trait variation matters in community ecology, Trends in Ecol. Evol. 26 (4) (2011) 183–192.
[12] S. Des Roches, D.M. Post, N.E. Turley, J.K. Bailey, A.P. Hendry, M.T. Kinnison, J.A. Schweitzer, E.P. Palkovacs, The ecological importance of intraspecific variation, Nature Ecol. Evol. 2 (1) (2018) 57–64.
[13] A. Sih, A. Bell, J.C. Johnson, Behavioral syndromes: an ecological and evolutionary overview, Trends in Ecol. Evol. 19 (7) (2004) 372–378.
[14] M. Wolf, F.J. Weissing, Animal personalities: consequences for ecology and evolution, Trends Ecol. Evol. 27 (8) (2012) 452–461.
[15] P.A. Schmidt, L.D. Mech, Wolf pack size and food acquisition, Am. Nat. 150 (4) (1997) 513–517.
[16] S. Creel, N.M. Creel, Communal hunting and pack size in African wild dogs, Lycaon pictus, Anim. Behav. 50 (5) (1995) 1325–1339.
[17] D.P. Hector, Cooperative hunting and its relationship to foraging success and prey size in an avian predator, Ethology 73 (3) (1986) 247–257.
[18] R. Bshary, A. Hohner, K. Ait-el Djoudi, H. Fricke, Interspecific communicative and coordinated hunting between groupers and giant moray eels in the red sea, PLoS Biol. 4 (12) (2006) e431.
[19] B.J. Toscano, B.D. Griffen, Trait-mediated functional responses: predator behavioural type mediates prey consumption, J. Anim. Ecol. 83 (6) (2014) 1469–1477.
[20] Y. Kuang, Delay Differential Equations: With Applications in Population Dynamics, 191, Academic press, 1993.
[21] H. Wang, J.D. Nagy, O. Gilg, Y. Kuang, The roles of predator maturation delay and functional response in determining the periodicity of predator–prey cycles, Math. Biosci. 221 (1) (2009) 1–10.
[22] P.J. Wangersky, W.J. Cunningham, Time lag in prey-predator population models, Ecology 38 (1) (1957) 136–139.
[23] S.A. Gourley, Y. Kuang, A stage structured predator-prey model and its dependence on maturation delay and death rate, J. Math. Biol. 49 (2) (2004) 188–200.
[24] M.Y. Li, X. Lin, H. Wang, Global Hopf branches and multiple limit cycles in a delayed Lotka-Volterra predator-prey model, Discr. Contin. Dyn. Syst.-B 19 (3) (2014) 747–760.
[25] H. Shu, W. Xu, Z. Hao, Global dynamics of an immunosuppressive infection model with stage structure, Mathe. Biosci. Eng. 17 (3) (2020) 2082–2102.
[26] S. Ahmed, X. Han, H. Wang, Behavioral plasticity in consumer-resource dynamics, SIAM J. Appl. Math. 85 (5) (2025) 2190–2214.

[27] M. Lu, J. Huang, H. Wang, An organizing center of codimension four in a predator-prey model with generalist predator: from tristability and quadristability to transients in a nonlinear environmental change, SIAM J. Appl. Dyn. Syst. 22 (2) (2023) 694–729.
[28] Z. Zhang, Qualitative Theory of Differential Equations, 101, American Mathematical Soc., 1992.
[29] Y. Zhang, J. Huang, H. Wang, Bifurcations driven by generalist and specialist predation: mathematical interpretation of Fennoscandia phenomenon, J. Math. Biol. 86 (6) (2023) 94.
[30] L. Perko, Differential Equations and Dynamical Systems, 7, Springer Science & Business Media, 2013.
[31] E. Beretta, Y. Kuang, Geometric stability switch criteria in delay differential systems with delay dependent parameters, SIAM J. Math. Anal. 33 (5) (2002) 1144–1165.
[32] J. Wu, Symmetric functional differential equations and neural networks with memory, Trans. Am. Math. Soc. 350 (12) (1998) 4799–4838.
[33] B.D. Hassard, N.D. Kazarinoff, Y.-H. Wan, Theory and Applications of Hopf Bifurcation, 41, CUP Archive, 1981.